

THE LONGITUDINAL DYNAMICS OF A RIGID AIRCRAFT
INCLUDING UNSTEADY AERODYNAMIC EFFECTS

by

Ta Kang Chen,,

Thesis submitted to the Graduate Faculty of the
Virginia Polytechnic Institute and State University
in partial fulfillment of the requirements for the degree of

MASTER OF SCIENCE

in

Aerospace and Ocean Engineering

APPROVED:

Dr. E. M. Cliff, Chairman

Dr. J. A. Schetz

Dr. F. H. Lutz, Jr.

September, 1977

Blacksburg, Virginia

ACKNOWLEDGMENTS

First and foremost the author wishes to express his appreciation to _____ who was the principal advisor for this thesis and whose encouragement, patience and breadth of knowledge made this study enjoyable. Thanks are due: to _____ and _____ for their kind advice and careful review of this work; to

_____ for all the help he rendered. The author especially wants to dedicate this thesis to his mother, _____. Without her love and sacrifice, the author could not have accomplished his educational goals.

TABLE OF CONTENTS

	Page
Acknowledgments	ii
Contents.	iii
List of Tables.	iv
List of Figures	v
Nomenclature.	vi
Introduction.	1
I. Problems of Non-Uniform Motion.	4
II. The Unsteady Aerodynamic Model.	14
III. Inclusion of the Unsteady Aerodynamics in the Aircraft Dynamic System.	19
IV. Inclusion of the Three-Dimensional Unsteady Aerodynamics in the Aircraft Dynamic System.	26
Conclusions	35
References.	37
Appendix 1.	39
Appendix 2.	42
Appendix 3.	43
Appendix 4.	45
Appendix 5.	48
Appendix 6.	49
Vita.	66

LIST OF TABLES

Table		Page
1	The Comparison Between the Approximated Transfer Function for Three-Dimensional Plunging Lift and the Data from H7WC	51
2	The Lift and Moment Coefficients in the Three-Dimensional Unsteady Motions	52
3	The Poles and Zeros of the Transfer Function in 2-D and 3-D Cases.	53
4	The Lift and Moment Coefficients in Three-Dimensional Sinusoidal Pure Pitching Motion.	54
5	The Eigenanalysis of Quasi-Steady System Matrix and Augmented System Matrices When Including Different Unsteady Aerodynamic Effects	55
6	Comparison of Some Useful Measures of the Rate of Growth or Decay of the Oscillation.	56

LIST OF FIGURES

Figure		Page
1.	The Flow Chart for the Two-Dimensional Lift Calculation. .	57
2.	The Bode Plot of the Lift Frequency Response in Two-Dimensional Case	58
3.	Sinusoidal Plunging Motion of the Airfoil in Two-Dimensional Case	59
4.	The Sinusoidal Plunging and Pitching Motion and Their Representations Used in the Program H7WC	60
5.	The Wing Geometry Used in the Program H7WC	61
6.	The Division of Strips and Boxes and Their Coordinates Used in the Program H7WC	62
7.	The Motion due to (a) Pitching Angle Change and (b) Angle of Attack Change	63
8.	The Rotary Oscillation in Free Flight Condition.	64
9.	The Block Diagram of Coupling the Unsteady Aerodynamics to the Quasi-Steady Aircraft System.	65

NOMENCLATURE

A	Dimensional system matrix
A_{ij}	Element of i^{th} row, j^{th} column in A
\hat{A}	Non-dimensional system matrix
AR	Aspect ratio
B	Dimensional control matrix
\hat{B}	Non-dimensional control matrix
b	Wing span
\bar{c}	Mean chord of airfoil
D	$\partial/\partial t$
$G_{ij}(s)$	Transfer function between input j and output i
g	gravity acceleration (32.17 ft/sec ²)
h	Vertical displacement from airfoil surface
$h_n \bar{c}$	Location of N. P. from leading edge
$h' \bar{c}$	Location of c.g. from leading edge
I_y	Pitching moment of inertia
\hat{I}_y	Non-dimensional pitching moment of inertia
i	$\sqrt{-1}$
K	Static gain
k	Reduced frequency ($= \frac{\omega \bar{c}}{2V}$)
L	Total lift
ΔL	Total lift change
l	Lift per unit span
Δl	Lift change per unit span
M	Total pitching moment

Ma	Mach number
m	Aircraft mass
$m_{L.E.}$	Pitching moment per unit span w.r.t. the leading edge
$m_{c.g.}$	Pitching moment per unit span w.r.t the c. g.
$\Delta m_{L.E.}$	Pitching moment change per unit span w.r.t. the L. E.
$\Delta m_{c.g.}$	Pitching moment change per unit span w.r.t. the c. g.
$N_{1/2}$	Cycles to half amplitude
p	Pole
q	Pitch rate
\hat{q}	Non-dimensional pitch rate
\bar{S}	Wing area
s	Semispan used in H7WC (in inches)
T	Transformation matrix between $\dot{\hat{x}}$ and \dot{x}
T^{-1}	Inverse matrix of T
T'	Transformation matrix between \hat{x} and x
ΔT	Thrust disturbance
t	Time
\hat{t}	$2V_e t/\bar{c}$
$t_{1/2}$	Time to half amplitude
u	Airfoil plunging velocity
u_0	Amplitude of sinusoidal plunging motion
V	Airspeed
\hat{V}	Non-dimensional airspeed
V_e	Reference airspeed
W	Airplane weight
x_a	Unknown aerodynamic state variable

x_L	Unknown aerodynamic state variable for lift part
x_M	Unknown aerodynamic state variable for moment part
x_i	Roots of cubic equation
\hat{x}	Non-dimensional state variable
$\dot{\hat{x}}$	$D\hat{x}/D\hat{t}$
z_i	zeros
α	Angle of attack
α_0	Amplitude of angle of attack variation
$\Delta\alpha$	Angle of attack disturbance
α_T	Thrust angle of attack
β_1	$\pi\bar{c}u_0$
γ_e	Reference flight path angle
γ	Flight path angle
$\Delta\gamma$	Disturbance of γ
ε	Camber ratio
Γ	Circulation
$\bar{\gamma}$	Strength of vortex sheet
ϕ	Potential of motion
$\Delta\phi$	Phase shift
θ	Pitch angle
θ_0	Amplitude of pitch angle variation
$\Delta\theta$	Disturbance in θ
ρ	Air density
$\hat{\mu}$	Non-dimensional mass ($= 2m/\rho\bar{S}\bar{c}$)
λ	$\omega\bar{c}/V$
λ'	Eigenvalues

ζ'	Damping ratio
ω	Damped circular frequency
ω_n	Natural frequency
C_m	Pitching moment coefficient
C_L	Lift coefficient
C_{L_e}	Lift coefficient at reference flight condition
C_{L_α}	$\partial C_L / \partial \alpha$
C_D	Drag coefficient
C_{D_α}	$\partial C_D / \partial \alpha$
C_{D_e}	Drag coefficient at reference flight condition
C_{m_α}	$\partial C_m / \partial \alpha$
C_{T_e}	Thrust coefficient at reference flight condition
C_W	$W / \frac{1}{2} \rho V^2 \bar{S}$
D_α	$\partial D / \partial \alpha$
L_q	$\partial L / \partial q$
L_V	$\partial L / \partial V$
L_α	$\partial L / \partial \alpha$
$L_{\dot{\alpha}}$	$\partial L / \partial \dot{\alpha}$
M_q	$\partial M / \partial q$
M_V	$\partial M / \partial V$
M_α	$\partial M / \partial \alpha$
$M_{\dot{\alpha}}$	$\partial M / \partial \dot{\alpha}$
T_e	Thrust at reference flight condition
T_V	$\partial T / \partial V$
$c_{m_q}^\wedge$	$\partial c_m / \partial q$
$c_{L_q}^\wedge$	$\partial c_L / \partial q$

Superscripts

- ' used in 2-D augmented system
- * used in 3-D augmented system

INTRODUCTION

There are various problems of practical aeronautics which require information on the aerodynamic pressures and forces acting on an airfoil in unsteady flight. Foremost among these are the problems of stability and control, followed by the phenomena of aeroelasticity, particularly, flutter. According to the classical theory of invicid incompressible flow, in the absence of free vortices, the pressure distribution on a rigid body depends only on the instantaneous velocities and accelerations of the body surface. This does not hold for wing theory, since a wing is usually followed by a vortex wake, and it is generally inapplicable to the motion of a body in a compressible fluid.

The classical theory of aircraft dynamics is based on Bryan's(ref. 1) representation of the aerodynamic forces acting on a body in flight. That is, each of the aerodynamic forces and moments is presumed to be uniquely determined at any time by the instantaneous values, and the derivatives, of the variables which define the motion and orientation of the body. Although this assumption is known to be valid only under special circumstances, the concept has been very successful when applied to a wide range of problems in aircraft dynamics. However, there are cases where it fails.

The basic limitation of the method of Bryan is its inability to account for the lagging mechanism of aerodynamic loads, i.e., the loads depend not only on the instantaneous motion but also its time history. In other words, Bryan's method has no "memory", so the conventional derivatives fail to give an accurate value of the instantaneous forces.

For example, a wing in subsonic flight leaves behind it a vortex wake of varying strength. The induced velocity field at the wing, which influences its lift, is dependent on the distribution of the circulation Γ all the way back to infinity, i.e. on the entire previous motion of the wing.

The two-dimensional potential theory of airfoils in nonuniform motion was first given by Wagner (ref. 2) and has been extended to problems involving the motion of hinged or flexible airfoils by Theodorsen (ref. 3) and Küssner (ref. 4). In the case of steady motion, a correction is known to be necessary before the results of the two-dimensional theory can be applied to wings of finite aspect ratio. A theory for the unsteady lift of finite wings was developed in reference 5. This theory has since been somewhat improved mathematically by using operational methods (ref. 6 and 7) in the solution of certain integral equations which arise.

While the development of practical, three-dimensional lifting-surface theories for flutter analysis throughout the various Mach number regimes was still beginning, Etkin (ref. 8 pp. 161-164) pointed out the usefulness of the theory of oscillating wings for calculating dynamic stability derivatives. Etkin demonstrated the calculation using Theodorsen's two-dimensional solution. And at that time, he found the difficulty that there is no Maclaurin series in the reduced frequency for the two-dimensional solution. Some other surveys have been done by Rodden and Revell (ref. 9) in 1962; by Ashley, Widnall and Landahl (ref. 10) in 1965 and by Landahl and Stark (ref. 11) in 1968.

Before Etkin's effort, M. Tobak first introduced the indicial function concept in the analysis of unsteady motions of wings (ref. 12).

He showed the qualitative variation of C_L with time for some α changes. By using the same concept, Etkin was able to introduce the aerodynamic transfer function idea on the stability derivatives for unsteady flight. Etkin's approach together with the numerical calculations of Rodden and Giesing (ref. 13) give the basis of our present analysis.

In constructing the unsteady aerodynamic model, an effort has been made to minimize the aerodynamic state variables required to describe the unsteady motion. Finally, the conventionally-used method, under the assumption of quasi-steady flight condition, has been evaluated in comparison with the results from the present unsteady aerodynamic model approach.

I. PROBLEMS OF NON-UNIFORM MOTION

Vortex System Associated with the Variations of the Circulation around an Airfoil

In this chapter most of the work is a version of Von Karman's work in Durand's book. For simplicity, we only briefly state the two-dimensional theory here. Those who are interested in the details can refer to reference 13, pp. 280~303.

It is true that in many cases the field of flow around an airfoil can be obtained with sufficient approximation by superposing the effects which are due to the influence of the angle of incidence and to the curvature, each considered separately. Extending this method to the present case, it may be assumed that to obtain an expression for the influence of the free vortices, it is sufficient to derive its value for the most simple type of airfoil; that is, for a flat plate lying in the horizontal plane.

It will be evident that in general every change of the state of motion of an airfoil will be accompanied by a change of the circulation Γ around it. Also for every change of Γ , a vortex must leave the trailing edge of the airfoil. The strength of this vortex is equal to the change of the circulation; the direction of rotation is opposite to that of the change in Γ . In the case of a continuously changing circulation, a continuous band of vortices develops behind the airfoil.

These phenomena account for the peculiar character of the problems of unsteady motion. The vortices which leave from the trailing edge produce a vertical component of velocity at the place of the airfoil, and so they have a marked influence upon the flow around the airfoil, and

thus upon the magnitude of the circulation.

Since the vortices are considered parallel to the span of the airfoil, the most important features of their influence are not affected by the restriction to the two-dimensional case. Now we shall suppose further that the general motion of the airfoil, considered with respect to the air at rest, is rectilinear, apart from oscillations of small amplitude in the vertical direction, which are considered in some problems.

If s is the distance travelled by the trailing edge of the airfoil in the direction of $-x$, measured from a given point of the x axis, then the velocity V is given by the equation

$$V = ds/dt \quad (1.1)$$

If in the interval from t to $t+dt$ the circulation around the airfoil changes by the amount $d\Gamma$, then from the trailing edge there separates a vortex of strength $-d\Gamma$. The strength $\bar{\gamma}$ of the vortex sheet (ref. 13, pp. 15) is

$$\bar{\gamma} = - \frac{d\Gamma}{ds} = - \frac{1}{V} \frac{d\Gamma}{dt} \quad (1.2)$$

Integration of (1.2) from $-\infty$ to s gives

$$\int_{-\infty}^s \bar{\gamma}(t, \xi) d\xi = - \Gamma(t, s) \quad (1.3)$$

The problems to be investigated now are the following:

1. In the first place we must find the influence of the vortices which constitute the band, upon the circulation around the airfoil. The problem can be solved, according to the treatment given by Wagner, by calculating the influence of a free vortex upon the flow around an airfoil with the aid of conformal transformation. The basic assumption

made in the calculation of the circulation is, as in the steady case, that its value at every moment produces tangential flow at the trailing edge. By combining (1.2) with the mathematical expression for the influence of the free vortices upon the circulation, a system of two equations is obtained, from which both Γ and $\bar{\gamma}$ can be determined.

2. After obtaining the circulation around the airfoil and the distribution of the vorticity in the wake, the next problem becomes the determination of the force and of the moment acting on the airfoil. This requires a special investigation, as the Kutta-Joukowski theorem in its usual form cannot be applied in the unsteady case.

Circulation around an Airfoil in the Presence of Free Vortices

Let V be the reference flight velocity, ρ the air density, \bar{c} the mean chord of the airfoil. If the airfoil is kept in a fixed position, then the lift per unit span is

$$l = 2\pi \cdot \frac{1}{2}\rho V^2 \bar{c} \cdot \alpha \quad (1.4)$$

and the circulation is

$$\Gamma = \pi \bar{c} V \alpha \quad (1.5)$$

1. If the airfoil is not at rest, but is making small vertical oscillations, the vertical velocity at any moment being u (reckoned positive downward), then the effective angle of incidence i is increased by the amount u/V ; hence we put:

$$i = \alpha + \frac{u}{V} \quad (1.6)$$

and instead of (1.5) we obtain the circulation due to this motion is

$$\Gamma' = \pi \bar{c} V \left(\alpha + \frac{u}{V} \right) = \pi \bar{c} (V\alpha + u) \quad (1.7)$$

2. The contribution due to the rotary oscillations is obtained by noting that a rotary motion about the center of the chord with the angular velocity $d\alpha / dt$ in the clockwise direction, imparts to the elements of the airfoil a normal velocity of the amount:

$$v_y = - \left(x + \frac{\bar{c}}{2} \right) \frac{d\alpha}{dt} \quad (1.8)$$

Rewrite $x = \bar{c}/2 \cdot (\cos\theta - 1)$ and according to Durand's book, the contribution of rotatory oscillations to the circulation is

$$\Gamma'' = \frac{\pi \bar{c}^2}{4} \frac{d\alpha}{dt} \quad (1.9)$$

3. Coming to the contribution to be derived from the presence of a free vortex, we assume, as indicated above, an airfoil in the form of a horizontal plate of breadth \bar{c} and consider an isolated vortex of strength Γ_1 at a distance ξ from the trailing edge. By means of the well known conformal transformation and method of images, the circulation around the airfoil due to this isolated vortex is

$$\Gamma_1 \left[\sqrt{\frac{\bar{c} + \xi}{\xi}} - 1 \right] \quad (1.10)$$

Replace the intensity Γ_1 of the vortex by $\bar{\gamma}(t, \xi) d\xi$, then the circulation due to the presence of the vortex system is

$$\Gamma''' = \int_0^{\infty} \bar{\gamma}(t, \xi) \left[\sqrt{\frac{\bar{c} + \xi}{\xi}} - 1 \right] d\xi \quad (1.11)$$

Adding together (1.7), (1.9), (1.11), we obtain the total circulation around the airfoil

$$\begin{aligned}\Gamma &= \Gamma' + \Gamma'' + \Gamma''' \\ &= \pi \bar{c} (V\alpha + u) + \frac{\pi \bar{c}^2}{4} \frac{d\alpha}{dt} + \int_0^\infty \bar{\gamma}(t, \xi) \left[\sqrt{\frac{\bar{c} + \xi}{\xi}} - 1 \right] d\xi\end{aligned}\quad (1.12)$$

This expression is valid both for the case of constant and for that of variable V .

Expressions for the Force and the Moment Acting upon the Airfoil

First we introduce the potential ϕ of the motion around the airfoil. Let the subscripts 1, 2 represent the lower and upper sides respectively, then the force per unit area f on the airfoil is

$$f = \rho V \bar{\gamma}(t, \xi) + \rho \frac{\partial}{\partial t} (\phi_2 - \phi_1) \quad (1.13)$$

From the force per unit area f , we can get the lift and moment per unit span (with respect to the leading edge) like the following:

$$l = \int_{-\bar{c}}^0 f dx = \rho V \Gamma + \rho \frac{d}{dt} \int_{-\bar{c}}^0 (\phi_2 - \phi_1) dx \quad (1.14)$$

$$\begin{aligned}m &= \int_{-\bar{c}}^0 f \cdot (\bar{c} + x) dx \\ &= \rho V \int_{-\bar{c}}^0 \bar{\gamma} \cdot (x + \bar{c}) dx + \rho \frac{d}{dt} \int_{-\bar{c}}^0 (\phi_2 - \phi_1) (\bar{c} + x) dx\end{aligned}\quad (1.15)$$

Let

$$I = \int_{-\bar{c}}^0 (\phi_2 - \phi_1) dx \quad (1.16)$$

$$J = \int_{-\bar{c}}^0 (\phi_2 - \phi_1) \left(\frac{\bar{c}}{2} + x \right) dx \quad (1.17)$$

we get:

$$l = \rho V \Gamma + \rho \dot{I} \quad (1.18)$$

$$m = \rho V (\Gamma \bar{c} - I) + \rho \left(\frac{\bar{c}}{2} \dot{I} + \dot{J} \right) \quad (1.19)$$

In the same reference, I, J, have been calculated and are given by

$$I = \frac{\pi c^2}{4} (V\alpha - V\varepsilon + u) + \frac{\bar{c}}{2} \Gamma + \int_0^\infty \bar{\gamma} \left[\frac{\bar{c}}{2} + \xi - \bar{c}\xi + \xi^2 \right] d\xi \quad (1.20)$$

$$J = \frac{\pi c^3}{32} V\varepsilon + \frac{\bar{c}^2}{16} \Gamma + \frac{\pi c^4}{128} \dot{\alpha} + \int_0^\infty \bar{\gamma} \left[\frac{\bar{c}^2}{16} + \frac{\bar{c}\xi + \xi^2}{2} - \left(\frac{\bar{c}}{4} + \frac{\xi}{2} \right) \sqrt{\bar{c}\xi + \xi^2} \right] d\xi \quad (1.21)$$

So finally,

$$l = \rho \pi \bar{c} V (V\alpha + u) + \frac{\rho \pi \bar{c}^2}{4} (\alpha - \varepsilon) \dot{V} + \frac{\pi \bar{c}^2 \rho}{4} (2V\dot{\alpha} + \dot{u}) + \frac{\rho V \bar{c}}{2} \int_0^\infty \frac{\bar{\gamma}(t, \xi)}{\sqrt{\bar{c}\xi + \xi^2}} d\xi \quad (1.22)$$

and the moment m in the case of oscillating airfoil will be given later.

Calculation of the Forces Experienced by the Oscillating Airfoil at Constant Velocity

In the two-dimensional case we have considered both sinusoidal plunging and sinusoidal pitching motions. For brevity, we consider the details of the plunging motion only. In particular, we shall explain how one calculates the lift variation with the frequency of the oscillation. First let us assume

$$\alpha = 0$$

$$u = u_0 \sin \omega t$$

$$\Gamma = \Gamma_0 + \Gamma_1 \sin \omega t + \Gamma_2 \cos \omega t$$

$$l = l_0 + l_1 \sin \omega t + l_2 \cos \omega t$$

From (1.22) 1 becomes

$$1 = \pi \bar{c} \rho V u + \frac{\pi \rho \bar{c}^{-2}}{4} \dot{u} + \frac{\rho V \bar{c}}{2} \int_0^{\infty} \frac{\bar{\gamma}(t, \xi)}{\sqrt{c \xi + \xi^2}} d\xi \quad (1.23)$$

We further assume that

$$\pi \bar{c} \rho V u + \frac{\rho \pi \bar{c}^{-2}}{4} \dot{u} = c_0 + c_1 \sin \omega t + c_2 \cos \omega t \quad (1.24)$$

1. The first two terms in (1.12) are:

$$\begin{aligned} \pi \bar{c} (V \alpha + u) + \frac{\pi \bar{c}^{-2}}{4} \dot{\alpha} &= \pi \bar{c} u \\ &= \pi \bar{c} u_0 \sin \omega t = \beta_1 \sin \omega t \end{aligned} \quad (1.25)$$

$$2. \text{ Since } \bar{\gamma}(t, \xi) = -\frac{1}{V} \left(\frac{d\Gamma}{dt} \right)_{t - \frac{\xi}{V}} \quad (1.26)$$

and $\Gamma = \Gamma_0 + \Gamma_1 \sin \omega t + \Gamma_2 \cos \omega t$

we get

$$\begin{aligned} \bar{\gamma}(t, \xi) &= -\frac{\omega}{V} \left[\left(\Gamma_1 \sin \omega t + \Gamma_2 \cos \omega t \right) \sin \frac{\omega \xi}{V} \right. \\ &\quad \left. + \left(\Gamma_1 \cos \omega t - \Gamma_2 \sin \omega t \right) \cos \frac{\omega \xi}{V} \right] \end{aligned} \quad (1.27)$$

So the last term in Γ equation is:

$$\begin{aligned} &\int_0^{\infty} \bar{\gamma} \left[\sqrt{\frac{c + \xi}{\xi}} - 1 \right] d\xi \\ &= -\frac{\omega \bar{c}}{V} \left[S \left(\Gamma_1 \sin \omega t + \Gamma_2 \cos \omega t \right) + C \left(\Gamma_1 \cos \omega t - \Gamma_2 \sin \omega t \right) \right] \end{aligned} \quad (1.28)$$

where $C = \int_0^{\infty} \cos \lambda \xi_1 \left[\sqrt{\frac{1 + \xi_1}{\xi_1}} - 1 \right] d\xi_1 \quad (1.29)$

$$S = \int_0^{\infty} \sin \lambda \xi_1 \left[\sqrt{\frac{1 + \xi_1}{\xi_1}} - 1 \right] d\xi_1 \quad (1.30)$$

$$\lambda = \frac{\omega \bar{c}}{V} \quad \text{and } \xi_1 = \xi / \bar{c}$$

3. The circulation Γ becomes

$$\Gamma = \Gamma_0 + \Gamma_1 \sin \omega t + \Gamma_2 \cos \omega t$$

$$= \beta_1 \sin \omega t - \lambda \left[S(\Gamma_1 \sin \omega t + \Gamma_2 \cos \omega t) + C(\Gamma_1 \cos \omega t - \Gamma_2 \sin \omega t) \right] \quad (1.31)$$

So, $\Gamma_0 = 0$

$$\begin{cases} (1 + \lambda S) \Gamma_1 - \lambda C \Gamma_2 = \beta_1 \\ \lambda C \Gamma_1 + (1 + \lambda S) \Gamma_2 = 0 \end{cases} \quad (1.32)$$

which gives

$$\begin{cases} \Gamma_1 = A_1 \beta_1 \\ \Gamma_2 = A_2 \beta_2 \end{cases} \quad (1.33)$$

where

$$\begin{aligned} A_1 &= \frac{1 + \lambda S}{(1 + \lambda S)^2 + \lambda^2 C^2} \\ A_2 &= \frac{-\lambda C}{(1 + \lambda S)^2 + \lambda^2 C^2} \end{aligned} \quad (1.34)$$

4. Now we solve (1.23) for plunging motion with constant velocity:

$$1 = \pi \bar{c} \rho V u + \frac{\rho \pi \bar{c}^{-2}}{4} \dot{u} + \frac{\rho V \bar{c}}{2} \int_0^\infty \frac{\bar{\gamma}}{\sqrt{c\xi + \xi^2}} d\xi \quad (1.35)$$

From the assumption and (1.24), we get

$$\begin{cases} c_0 = 0 \\ c_1 = \rho \pi \bar{c} V u_0 \\ c_2 = \frac{\rho \pi \bar{c} u_0 V}{4} \lambda \end{cases} \quad (1.36)$$

Using (1.27), we now have another two integrals:

$$P = \int_0^{\infty} \cos \lambda \xi_1 \frac{1}{\sqrt{\xi_1^2 + \xi_1}} d\xi_1 \quad (1.37)$$

$$Q = \int_0^{\infty} \sin \lambda \xi_1 \frac{1}{\sqrt{\xi_1^2 + \xi_1}} d\xi_1 \quad (1.38)$$

5. The final form for l is

$$\left\{ \begin{array}{l} l_0 = 0 \\ l_1 = c_1 + \frac{\rho V \lambda}{2} (-Q\Gamma_1 + P\Gamma_2) \\ l_2 = c_2 + \frac{\rho V \lambda}{2} (-P\Gamma_1 - Q\Gamma_2) \end{array} \right. \quad (1.39)$$

The flow chart of the computer program in calculating the two-dimensional case is given in Figure 1. So from the above equations (1.23)-(1.39) and a given plunging velocity amplitude u_0 , we can calculate both the in-phase and out-of-phase parts of unsteady lift easily. By the same method, we can get the unsteady lift for pitching motion (actually, the rotary oscillation) easily.

Two-dimensional Unsteady Moment Part

From Durand's work (pp. 303(c)),

$$m_{L.E.} = - \left\{ \frac{\bar{c}l}{4} + \left[\frac{\pi \bar{c}^2}{4} \rho V^2 \epsilon + \frac{\pi \bar{c}^3}{16} (2\rho V \dot{\alpha} + \rho \dot{u}) + \frac{\pi \bar{c}^4}{128} \rho \ddot{\alpha} \right] \right\} \quad (1.40)$$

This moment is calculated with respect to the leading edge. Theoretically, the moment taken with respect to the $\bar{c}/4$ point from the leading edge is independent of the vorticity of the wake and thus of the past history, so the terms in the bracket is a constant of time.

Change $m_{L.E.}$ to $m_{c.g.}$

Suppose the center of gravity is $h'\bar{c}$ from the leading edge, then

$$m_{c.g.} = - \left\{ \left(\frac{1}{4} - h' \right) \bar{c} l + \left[\frac{\pi \bar{c}^{-2}}{4} \rho V^2 \epsilon + \frac{\pi \bar{c}^{-3}}{16} (2\rho V \dot{\alpha} + \rho \dot{u}) + \frac{\pi \bar{c}^{-4}}{128} \rho \ddot{\alpha} \right] \right\} \quad (1.41)$$

Let $m_{c.g.}$ be the change of moment about center of gravity due to the unsteady motion, then we have

$$\Delta m_{c.g.} = - \left(\frac{1}{4} - h' \right) \bar{c} (\Delta l) \quad (1.42)$$

$$\text{or } \Delta M_{c.g.} = - \left(\frac{1}{4} - h' \right) \bar{c} (\Delta L) \quad (1.43)$$

II. THE UNSTEADY AERODYNAMIC MODEL

System Identification of the Unsteady Lift Frequency Response

By using the computer algorithm in Chapter 1 and given the values of \bar{c} , V , u_0 , ρ , we are able to calculate the lift of the airfoil corresponding to the sinusoidal plunging and pitching motions of different frequencies. The Bode plot of this two-dimensional frequency response is shown in Figure 2 for plunging motion.

Now that we have found the frequency response of the unsteady lift, the next important thing is to find the transfer function which characterizes this frequency response. There are many papers (ref. 14-17) discussing this subject, most of them use computer aid in finding the transfer function. Because this is not the main topic of this thesis, we are not going deeply into the discussion and comparison of these different existing methods. But for our case, it looks very possible that there are one pole and two zeros for the unsteady lift transfer function as we can verify later. For this situation, we are able to use a simple but precise enough method to find the locations of the poles and zeros. For the frequency range we are most interested in ($k < 0.05$), the error of the result from this method compared with the data is well below 0.1% (see Table 1). Because of this success, we will use the same method all through this analysis. This method is illustrated in Appendix 1, the finding of the transfer function from known poles and zeros is in Appendix 2 and an example case is given in Appendix 3.

By using the method depicted in Appendix 1, 2, we get one pole and two zeros as expected for transfer function representing two-dimensional

plunging motion:

$$p = 5.90209$$

$$z_1 = 9.00983$$

$$z_2 = 182.23874$$

The transfer function between the input u , where $u = \text{Re}(u_0 e^{i\omega t})$ and $u_0 = 1 \text{ ft/sec}$, and the output lift coefficient C_L is:

$$G_{C_L u}(s) = 0.008446 \frac{0.000609 s^2 + 0.11648 s + 1}{0.16943 s + 1} \quad (2.1)$$

$$G_{C_L \dot{u}}(s) = \frac{1}{s} G_{C_L u}(s) = 0.008446 \frac{0.000609 s^2 + 0.11648 s + 1}{s(0.16943 s + 1)} \quad (2.2)$$

Similarly, we can get the transfer function for pitching motion and this is given in Chapter 3.

Unsteady Part of the Lift

The above transfer function is actually for the total lift coefficient variation with respect to the frequency, not the lift coefficient difference between the steady case and the unsteady case with respect to the frequency. So before we can apply the transfer function to the aircraft system, we need to find the transfer function for the lift coefficient change from the steady condition with respect to the frequency. First we find the static gain of the total lift coefficient transfer function:

$$\text{Static gain } K = \lim_{s \rightarrow 0} s \cdot G(s) = 0.008446 \quad (2.3)$$

Let L represent the total lift at a given flight condition, u is the velocity perpendicular to the airfoil (Fig. 3), $G_{L \dot{u}}(s)$ is the transfer function for the total lift and $G_{\Delta L \dot{u}}(s)$ is the unsteady part of lift due

to the plunging motion. Then

$$\begin{aligned} G_{\Delta L \dot{u}}(s) &= G_{L \dot{u}}(s) - \text{total lift at reference flight condition} \\ &= G_{L \dot{u}}(s) - \frac{K}{s} \end{aligned}$$

Suppose the total lift transfer function is written in the following form:

$$G_{L \dot{u}}(s) = \frac{K (T_2 s^2 + T_3 s + 1)}{s (T_1 s + 1)} \quad (2.4)$$

then

$$G_{\Delta L \dot{u}}(s) = G_{L \dot{u}}(s) - \frac{K}{s} = K \frac{T_2 s^2 + (T_3 - T_1) s + 1}{T_1 s + 1} \quad (2.5)$$

Realization of the Transfer Function

For quasi-steady case, the aircraft dynamic system is given by

$$\dot{x} = A x + B \delta \quad (2.6)$$

where $x = [\Delta V, \Delta \alpha, q, \Delta \theta]^T$ and A characterize forces and moments. But in quasi-steady flight condition,

$$Z(t) = Z_\alpha \cdot \alpha(t) + Z_q \cdot q(t) + Z_\delta \cdot \delta(t) + \dots \quad (2.7)$$

which is not true for unsteady motion. So we want to seek a model, having a form of

$$\begin{cases} \dot{x}_a(t) = a x_a(t) + b \dot{u}(t) \\ Z(t) = c x_a(t) + d \dot{u}(t) \end{cases} \quad (2.8)$$

which can accurately represent the same frequency response as the present transfer function does. This lies in the category of realization problem,

which is discussed in Brogan's book (ref. 14). From (2.5), we can see that this transfer function actually represents a first-order system:

Let us write it in this form:

$$\begin{cases} \dot{x} = a' x + \dot{u} \\ \Delta L = c_1' x + d_1' \dot{u} \end{cases} \quad (2.9)$$

When u is small compared with V_e , i.e. $u \ll V_e$,

$$u = V_e \tan \alpha \approx V_e \alpha \quad (2.10)$$

So, from equation (2.9),

$$\dot{u} = V_e \dot{\alpha} + \alpha \dot{V} \approx V_e \dot{\alpha} \quad (2.11)$$

Here we have neglected $\alpha \dot{V}$ term, because both α_e and \dot{V} are small compared to the first term. Rewrite (2.9), we get the unsteady aerodynamic model for the plunging motion lift part:

$$\begin{cases} \dot{x} = a' x + V_e \dot{\alpha} \\ \Delta L = c_1' x + d_1' \dot{\alpha} \end{cases} \quad (2.12)$$

where $d_1' = V_e \cdot d_1$

After identifying the parameters, we get

$$\begin{aligned} a' &= -\frac{1}{T_1} \\ c_1' &= \frac{K}{T_1} \left(T_3 - T_1 - \frac{T_2}{T_1} \right) \\ d_1' &= \frac{V_e K T_2}{T_1} \end{aligned} \quad (2.13)$$

Construction of the whole Unsteady Aerodynamic Model

Now we have found the model for the lift part, but it is still not

complete. In order to include the moment change due to the unsteady motion into account, we must return to equation (1.43):

$$\Delta M_{c.g.} = - \left(\frac{1}{4} - h' \right) \bar{c} (\Delta L) \quad (2.14)$$

Combine (1.43) and (2.12), we get

$$\Delta M_{c.g.} = \left(h' - \frac{1}{4} \right) \bar{c} \{ c_1' x + d_1' \dot{\alpha} \} \quad (2.15)$$

Since the unsteady aerodynamics influence is mostly in the aircraft's body Z-axis direction, so we will ignore the ΔX . From (2.12), (2.13) and (2.15), the complete unsteady aerodynamic model looks like:

$$\begin{aligned} \dot{x} &= - \frac{1}{T_1} x + V_e \cdot \dot{\alpha} \\ \left\{ \begin{array}{c} \Delta L \\ \Delta M_{c.g.} \end{array} \right\} &= \left[\begin{array}{c} \frac{K}{T_1} \left(T_3 - T_1 - \frac{T_2}{T_1} \right) \\ \left(h' - \frac{1}{4} \right) \frac{\bar{c}K}{T_1} \left(T_3 - T_1 - \frac{T_2}{T_1} \right) \end{array} \right] x + \left[\begin{array}{c} \frac{V_e K T_2}{T_1} \\ \left(h' - \frac{1}{4} \right) \frac{\bar{c} V_e K T_2}{T_1} \end{array} \right] \dot{\alpha} \end{aligned} \quad (2.16)$$

III. INCLUSION OF THE UNSTEADY AERODYNAMICS TO
THE AIRCRAFT DYNAMIC SYSTEM

The Quasi-steady Aircraft Dynamic System

In this chapter we will follow the notation used by Etkin (ref.15). The quasi-steady longitudinal equations are given by equation(5.10,24) for dimensional case, and by (5.13,19) for non-dimensional case in reference 15. Let $x = [\Delta V, \Delta\alpha, q, \Delta\theta]^T$, then (5.10,24) can be written as

$$\dot{x}(t) = A x(t) \quad (3.1)$$

where A is the quasi-steady system matrix, a_{ij} is the ith row, jth column element and the sixteen elements are listed below as reference for use later.

$$A_{11} = \frac{T_V \cos \alpha_T - D_V}{m} \quad (3.2-1)$$

$$A_{12} = g \cos \gamma_e - \frac{D_\alpha + T_e \sin \alpha_T}{m} \quad (3.2-2)$$

$$A_{13} = 0 \quad (3.2-3)$$

$$A_{14} = -g \cos \gamma_e \quad (3.2-4)$$

$$A_{21} = - \frac{L_V + T_V \sin \alpha_T}{mV_e + L_\dot{\alpha}} \quad (3.2-5)$$

$$A_{22} = - \frac{L_\alpha + T_e \cos \alpha_T - mg \sin \gamma_e}{mV_e + L_\dot{\alpha}} \quad (3.2-6)$$

$$A_{23} = \frac{mV_e - L_q}{mV_e + L_\dot{\alpha}} \quad (3.2-7)$$

$$A_{24} = - \frac{mg \sin \gamma_e}{mV_e + L_\dot{\alpha}} \quad (3.2-8)$$

$$A_{31} = \frac{1}{I_y} \left[M_V - M_{\dot{\alpha}} \frac{L_V + T_V \sin \alpha_T}{mV_e + L_{\dot{\alpha}}} \right] \quad (3.2-9)$$

$$A_{32} = \frac{1}{I_y} \left[M_{\alpha} - \frac{M_{\dot{\alpha}} (L_{\alpha} + T_e \cos \alpha_T - mgsin \gamma_e)}{mV_e + L_{\dot{\alpha}}} \right] \quad (3.2-10)$$

$$A_{33} = \frac{1}{I_y} \left[M_q + \frac{M_{\dot{\alpha}} (mV_e - L_q)}{mV_e + L_{\dot{\alpha}}} \right] \quad (3.2-11)$$

$$A_{34} = \frac{1}{I_y} \left[- \frac{M_{\dot{\alpha}} mgsin \gamma_e}{mV_e + L_{\dot{\alpha}}} \right] \quad (3.2-12)$$

$$A_{41} = 0 \qquad A_{42} = 0 \quad (3.2-13)$$

$$A_{43} = 1 \qquad A_{44} = 0$$

The Aircraft Dynamic System When Including the Unsteady Aerodynamic Model

The aerodynamic force model used in Etkin's formation is quasi-steady. Thus, the lift force, L , is assumed to vary as

$$L(t) = L_V \Delta V(t) + \dots \quad (3.3)$$

This accounts for the presence of the stability derivatives L_V , L_{α} , etc. in the listed expressions for the a_{ij} elements above. We now want to add in the effect of unsteady aerodynamics as predicted by our realization model. Most simply this is done by retaining to the dynamic equations and considering each force component as a sum of quasi-steady term, and an unsteady contribution. For example, the lift is

$$L(t) = L_{qs}(t) + \Delta L(t)$$

where $L_{qs}(t)$ is the quasi-steady form (2.7) and $\Delta L(t)$ is the unsteady part derived in Chapter 2.

Since $L(\cdot)$ is modeled as the output of a first order system, it is

necessary to add a fifth state variable to the previous model. The new elements of the fifth-order system are listed below, and the derivations of these elements are given in Appendix 4. We name the extra unknown aerodynamic state variable x_a . The result is a model with $x' = [\Delta V, \Delta \alpha, q, \Delta \theta, x_a]^T$ and

$$\dot{x}' = A' x'(t) \quad (3.5)$$

$$A'_{11} \sim A'_{14} \text{ are the same as } A_{11} \sim A_{14}. \quad (3.6-1)$$

$$A'_{15} = 0$$

$$A'_{21} = - \frac{L_V + T_V \sin \alpha_T}{mV_e + d'_1} \quad (3.6-2)$$

$$A'_{22} = - \frac{T_e \cos \alpha_T - mg \sin \gamma_e + L_\alpha}{mV_e + d'_1} \quad (3.6-3)$$

$$A'_{23} = \frac{mV_e - L_q}{mV_e + d'_1} \quad (3.6-4)$$

$$A'_{24} = - \frac{mg \sin \gamma_e}{mV_e + d'_1} \quad (3.6-5)$$

$$A'_{25} = - \frac{c'_1}{mV_e + d'_1} \quad (3.6-6)$$

$$A'_{31} = \frac{1}{I_y} \left[M_V - \frac{d'_2 (L_V + T_V \sin \alpha_T)}{mV_e + d'_1} \right] \quad (3.6-7)$$

$$A'_{32} = \frac{1}{I_y} \left[M_\alpha - \frac{d'_2 (L_\alpha + T_e \cos \alpha_T - mg \sin \gamma_e)}{mV_e + d'_1} \right] \quad (3.6-8)$$

$$A'_{33} = \frac{1}{I_y} \left[M_q + \frac{d'_2 (mV_e - L_q)}{mV_e + d'_1} \right] \quad (3.6-9)$$

$$A'_{34} = \frac{1}{I_y} \left[- \frac{d'_2 (mg \sin \gamma_e)}{mV_e + d'_1} \right] \quad (3.6-10)$$

$$A'_{35} = \frac{1}{I_y} \left[c'_2 - \frac{d'_2 \cdot c'_1}{mV_e + d'_1} \right] \quad (3.6-11)$$

$$A'_{41} \sim A'_{44} \text{ are the same as } A_{41} \sim A_{44}.$$

$$A'_{45} = 0 \quad (3.6-12)$$

$$A'_{51} = V_e A'_{21} \quad (3.6-13)$$

$$A'_{52} = V_e A'_{22} \quad (3.6-14)$$

$$A'_{53} = V_e A'_{23} \quad (3.6-15)$$

$$A'_{54} = V_e A'_{24} \quad (3.6-16)$$

$$A'_{55} = a' + V_e A'_{25} \quad (3.6-17)$$

Comparison of the New Model with the Conventional Model

Compare equation (3.6) with equation (3.2), we find that L_{α} has been changed to d'_1 and M_{α} to d'_2 . Since we ignored the influence on the X-direction force, the first row of A' remains unchanged as compared with A . The elements in fifth column and fifth row are new and they give the different shape to the initial system matrix.

Numerical Example

For the purpose of determining what the influence of unsteady aerodynamics on the aircraft longitudinal dynamic system, we use the example given in Etkin (ref. 14, pp. 320-328). We make the same assumption as in the book, i.e. $\gamma_e = \alpha_T = 0$, and use the unsteady aerodynamic model derived from a rigid wing experiencing sinusoidal plunging motion and pitching motion respectively. At present, we simply consider the contribution from the wing only instead of the wing-body-tail combination. In Chapter 4, we will consider the three-dimensional condition which will better illustrate the influence of the unsteady aerodynamics on the long-

gitudinal modes of the example aircraft. The data which pertains to a hypothetical jet transport airplane flying at high altitude is given in Appendix 5.

Using the linear transformation from non-dimensional case to dimensional case (Appendix 6), we have

$$\begin{pmatrix} \dot{v} \\ \dot{\alpha} \\ \dot{q} \\ \dot{\theta} \end{pmatrix} = \begin{bmatrix} -0.00658 & 17.83112 & 0.0 & -32.17 \\ -0.00012 & -0.85731 & 1.0 & 0.0 \\ 0.00003 & -3.30544 & -1.35549 & 0.0 \\ 0.0 & 0.0 & 1.0 & 0.0 \end{bmatrix} \begin{pmatrix} \Delta V \\ \Delta \alpha \\ q \\ \Delta \theta \end{pmatrix} \quad (3.7)$$

1. The two-dimensional augmented longitudinal dynamics when including the unsteady aerodynamics of plunging motion only:

Now we couple the unsteady aerodynamics of plunging motion to the quasi-steady case. Using the method in Chapter 2, the transfer function for the two-dimensional unsteady lift is

$$G_{\Delta L \dot{u}}(s) = 3362.53 \frac{0.0035944 s - 0.31252}{s + 5.90209} \quad (3.8)$$

The unsteady aerodynamic model in state space form is

$$\begin{aligned} \dot{x}_a &= -5.90209 x_a + 733 \dot{\alpha} \\ \begin{pmatrix} \Delta L \\ \Delta M_{c.g.} \end{pmatrix} &= \begin{bmatrix} -1122.19 \\ 2013.32 \end{bmatrix} x_a + \begin{bmatrix} 8859.26 \\ -15894.39 \end{bmatrix} \dot{\alpha} \end{aligned} \quad (3.9)$$

Following (3.6), we have the 5x5 augmented longitudinal system matrix as given in (3.10). The eigenanalysis is given in Table 5 and Table 6 for the system matrix including unsteady aerodynamics. The quasi-steady case is also listed for comparison.

$$\begin{bmatrix} -0.00658 & 17.83112 & 0.0 & -32.17 & 0.0 \\ -0.00012 & -0.85398 & 0.99612 & 0.0 & 0.00049 \\ 0.0 & -3.47498 & -1.15767 & 0.0 & 0.00156 \\ 0.0 & 0.0 & 1.0 & 0.0 & 0.0 \\ -0.08796 & -625.96734 & 730.15596 & 0.0 & -5.54292 \end{bmatrix} \quad (3.10)$$

2. The two-dimensional augmented longitudinal dynamics when including the unsteady aerodynamics of pitching motion (rotary oscillation) only:

The transfer function for the two-dimensional unsteady lift is

$$G_{L\dot{\alpha}}(s) = 43148.38 \frac{0.00076414 s^2 + 0.11927 s + 1}{s(0.15774 s + 1)} \quad (3.11)$$

The unsteady aerodynamic model in state space form is

$$\begin{aligned} \dot{x} &= -6.33966 x + \dot{\alpha} \\ \begin{Bmatrix} \Delta L \\ \Delta M_{c.g.} \end{Bmatrix} &= \begin{bmatrix} -11848.24 \\ 21256.93 \end{bmatrix} x + \begin{bmatrix} 209.02 \\ -375.01 \end{bmatrix} \dot{\alpha} \end{aligned} \quad (3.12)$$

The augmented longitudinal system matrix is

$$\begin{bmatrix} -0.00658 & 17.83112 & 0.0 & -32.17 & 0.0 \\ -0.00012 & -0.85723 & 0.99982 & 0.0 & 0.00521 \\ 0.0 & -3.48531 & -1.14567 & 0.0 & 0.0165 \\ 0.0 & 0.0 & 1.0 & 0.0 & 0.0 \\ -0.00012 & -0.85725 & 0.99982 & 0.0 & -6.33445 \end{bmatrix} \quad (3.13)$$

Short Discussion

In Table 5, we have listed the eigenanalysis of both the quasi-steady-

dy and unsteady motion cases. As we can see, when we take the unsteady aerodynamics into account, both the short period and phugoid modes have changed somewhat. Both modes tend to be destabilized, depending on which motion is taken into account. The unsteady aerodynamics from the plunging motion tends to affect the short period mode more than it affects the phugoid mode. For either aerodynamic model (plunging or pitching), the phugoid mode remains essentially the same.

IV. INCLUSION OF THE THREE-DIMENSIONAL UNSTEADY AERODYNAMICS TO THE AIRCRAFT DYNAMIC SYSTEM

The Application of Computer Program H7WC (ref. 15)

In the three-dimensional case, J. P. Giesing, T.P. Kalman and W. P. Rodden's computer program H7WC has been used for both plunging and pitching motions. The calculations are carried out using the oscillatory lifting-surface method described in reference 16 which is based on the Doublet Lattice Method of Albano and Rodden (ref. 17). For illustration, the shape of the sinusoidal plunging and pitching motions are given in Figure 4. The program H7WC requires a specified wing geometry as part of its input. The wing planform used is given in Figure 5 for completeness. The detailed specifications are shown in the following Figure 6. The pitching motion here is with respect to the wind axes. The results are for $u_0 = 1$ ft/sec for plunging motion and 1° pitching angle for pitching motion only. Some of the lift and moment coefficients for plunging and pitching motion of the example jet transport's wing at a Mach number of 0.737 are shown in Table 2. Using the same method as in the two-dimensional case, we get the poles and zeros for the transfer functions and they are listed in Table 3.

The Three-Dimensional Unsteady Aerodynamic Model

In three-dimensional case, the system realization will be somewhat different from the two-dimensional case even though the identification procedure is still the same. Usually, the unsteady lift transfer function and the unsteady moment transfer function will have different pole positions. Thus for plunging motion we have:

$$\begin{cases} \dot{x}_L = a'_L x_L + V_e \cdot \dot{\alpha} \\ \Delta L = c'_1 x_L + d'_1 \dot{\alpha} \end{cases} \quad (4.1)$$

$$\begin{cases} \dot{x}_M = a'_M x_M + V_e \cdot \dot{\alpha} \\ \Delta M = c'_2 x_M + d'_2 \dot{\alpha} \end{cases} \quad (4.2)$$

and for pitching motion:

$$\begin{cases} \dot{x}_L = a'_L x_L + 1 \cdot \dot{\alpha} \\ \Delta L = c'_1 x_L + \frac{d'_1}{V_e} \dot{\alpha} \end{cases} \quad (4.3)$$

$$\begin{cases} \dot{x}_M = a'_M x_M + 1 \cdot \dot{\alpha} \\ \Delta M = c'_2 x_M + \frac{d'_2}{V_e} \dot{\alpha} \end{cases} \quad (4.4)$$

where each of the above a'_L , c'_1 , d'_1 , a'_M , c'_2 , d'_2 comes from each part of the motion's realization procedure as depicted in Chapter 2. Let

$$\begin{aligned} a_{11}^* &= a'_L & a_{22}^* &= a'_M \\ c_{11}^* &= c'_1 & c_{22}^* &= c'_2 \\ d_1^* &= d'_1 & d_2^* &= d'_2 \end{aligned} \quad (4.5)$$

then the three-dimensional unsteady aerodynamic model for the plunging motion is

$$\begin{cases} \dot{x}_L \\ \dot{x}_M \end{cases} = \begin{bmatrix} a_{11}^* & 0 \\ 0 & a_{22}^* \end{bmatrix} \begin{cases} x_L \\ x_M \end{cases} + \begin{bmatrix} V_e \\ V_e \end{bmatrix} \dot{\alpha}$$

$$\begin{cases} \Delta L \\ \Delta M \end{cases} = \begin{bmatrix} c_{11}^* & 0 \\ 0 & c_{22}^* \end{bmatrix} \begin{cases} x_L \\ x_M \end{cases} + \begin{bmatrix} d_1^* \\ d_2^* \end{bmatrix} \dot{\alpha} \quad (4.6)$$

and for pitching motion:

$$\begin{aligned} \begin{Bmatrix} \dot{x}_L \\ \dot{x}_M \end{Bmatrix} &= \begin{bmatrix} a_{11}^* & 0 \\ 0 & a_{22}^* \end{bmatrix} \begin{Bmatrix} x_L \\ x_M \end{Bmatrix} + \begin{bmatrix} 1 \\ 1 \end{bmatrix} \dot{\alpha} \\ \begin{Bmatrix} \Delta L \\ \Delta M \end{Bmatrix} &= \begin{bmatrix} c_{11}^* & 0 \\ 0 & c_{22}^* \end{bmatrix} \begin{Bmatrix} x_L \\ x_M \end{Bmatrix} + \begin{bmatrix} d_1^*/v_e \\ d_2^*/v_e \end{bmatrix} \dot{\alpha} \end{aligned} \quad (4.7)$$

The Three-Dimensional Augmented Systems

The augmented systems derived from (4.6) and (4.7) are of order six which is one order higher than the two-dimensional idealized case. Now the six state variables are ΔV , $\Delta \alpha$, q , $\Delta \theta$, x_L , x_M , and the elements of the augmented system for each motion are given below.

1. System matrix elements for plunging motion (4.8):

$$\begin{aligned} A_{11}^* &= A_{11}' & A_{12}^* &= A_{12}' \\ A_{13}^* &= A_{13}' & A_{14}^* &= A_{14}' \\ A_{15}^* &= 0 & A_{16}^* &= 0 \\ A_{21}^* &= A_{21}' & A_{22}^* &= A_{22}' \\ A_{23}^* &= A_{23}' & A_{24}^* &= A_{24}' \\ A_{25}^* &= -\frac{c_{11}^*}{d_1^* + mV_e} & A_{26}^* &= 0 \\ A_{31}^* &= A_{31}' & A_{32}^* &= A_{32}' \\ A_{33}^* &= A_{33}' & A_{34}^* &= A_{34}' \end{aligned}$$

$$\begin{aligned}
 A_{35}^* &= -\frac{1}{I_y} \left[\frac{d_2^* c_{11}^*}{d_1^* + mV_e} \right] & A_{36}^* &= \frac{c_{22}^*}{I_y} \\
 A_{41}^* &= 0 & A_{42}^* &= 0 \\
 A_{43}^* &= 1 & A_{44}^* &= 0 \\
 A_{45}^* &= 0 & A_{46}^* &= 0 \\
 A_{51}^* &= A_{51}' & A_{52}^* &= A_{52}' \\
 A_{53}^* &= A_{53}' & A_{54}^* &= A_{54}' \\
 A_{55}^* &= a_{11}^* - \frac{V_e c_{11}^*}{mV_e + d_1^*} & A_{56}^* &= 0 \\
 A_{61}^* &= A_{51}' & A_{62}^* &= A_{52}' \\
 A_{63}^* &= A_{53}' & A_{64}^* &= A_{54}' \\
 A_{65}^* &= V_e A_{25}^* & A_{66}^* &= a_{22}^*
 \end{aligned}$$

2. System matrix elements for pitching motion (4.9):

$$\begin{aligned}
 A_{11}^* &= A_{11}' & A_{12}^* &= A_{12}' \\
 A_{13}^* &= A_{13}' & A_{14}^* &= A_{14}' \\
 A_{15}^* &= 0 & A_{16}^* &= 0 \\
 A_{21}^* &= A_{21}' & A_{22}^* &= A_{22}' \\
 A_{23}^* &= A_{23}' & A_{24}^* &= A_{24}' \\
 A_{25}^* &= -\frac{V_e c_{11}^*}{d_1^* + mV_e} & A_{26}^* &= 0
 \end{aligned}$$

$$\begin{aligned}
 A_{31}^* &= A_{31}' & A_{32}^* &= A_{32}' \\
 A_{33}^* &= A_{33}' & A_{34}^* &= A_{34}' \\
 A_{35}^* &= -\frac{1}{I_y} \left[\frac{V_e c_{11}^*}{d_1^* + mVe} \right] & A_{36}^* &= \frac{c_{22}^*}{I_y} \\
 A_{41}^* &= 0 & A_{42}^* &= 0 \\
 A_{43}^* &= 1 & A_{44}^* &= 0 \\
 A_{45}^* &= 0 & A_{46}^* &= 0 \\
 A_{51}^* &= A_{21}' & A_{52}^* &= A_{22}' \\
 A_{53}^* &= A_{23}' & A_{54}^* &= A_{24}' \\
 A_{55}^* &= a_{11}^* + A_{25}^* & A_{56}^* &= 0 \\
 A_{61}^* &= A_{21}' & A_{62}^* &= A_{22}' \\
 A_{63}^* &= A_{23}' & A_{64}^* &= A_{24}' \\
 A_{65}^* &= A_{25}^* & A_{66}^* &= a_{22}^*
 \end{aligned}$$

Numerical Example

Assume the same reference flight condition as in the two-dimensional case and consider a rigid wing and the contribution from the wing only.

1. The three-dimensional unsteady aerodynamic model for the plunging motion:

a. 3-D plunging motion lift transfer function:

$$G_{C_L \dot{u}}(s) = 0.008285 \frac{0.00018291 s^2 + 0.050547 s + 1}{s(0.070576 s + 1)} \quad (4.10)$$

$$G_{L\dot{u}}(s) = 3298.43 \frac{0.00018291 s^2 + 0.050547 s + 1}{s(0.070576 s + 1)} \quad (4.11)$$

$$\begin{cases} \dot{x}_L = -14.17 x_L + 733 \dot{\alpha} \\ \Delta L = -1057.20 x_L + 6266.02 \dot{\alpha} \end{cases} \quad (4.12)$$

b. 3-D plunging motion moment transfer function:

$$G_{C_M\dot{u}}(s) = -0.00465 \frac{0.00031097 s^2 + 0.057819 s + 1}{s(0.073842 s + 1)} \quad (4.13)$$

$$G_{M\dot{u}}(s) = -28509.46 \frac{0.00031097 s^2 + 0.057819 s + 1}{s(0.073842 s + 1)} \quad (4.14)$$

$$\begin{cases} \dot{x}_M = -13.54 x_M + 733 \dot{\alpha} \\ \Delta M = 7812.20 x_M - 88005.13 \dot{\alpha} \end{cases} \quad (4.15)$$

The combined unsteady aerodynamic model for the three-dimensional plunging motion with amplitude $u_0 = 1$ ft/sec is written as:

$$\begin{cases} \dot{x}_L \\ \dot{x}_M \end{cases} = \begin{bmatrix} -14.17 & 0 \\ 0 & -13.54 \end{bmatrix} \begin{cases} x_L \\ x_M \end{cases} + \begin{bmatrix} 733 \\ 733 \end{bmatrix} \dot{\alpha} \quad (4.16)$$

$$\begin{cases} \Delta L \\ \Delta M \end{cases} = \begin{bmatrix} -1057.20 & 0 \\ 0 & 7812.20 \end{bmatrix} \begin{cases} x_L \\ x_M \end{cases} + \begin{bmatrix} 6266.02 \\ -88005.13 \end{bmatrix} \dot{\alpha}$$

2. The three-dimensional unsteady aerodynamic model for the pitching motion:

a. 3-D pitching motion lift transfer function:

$$G_{C_L\dot{\alpha}}(s) = 0.10603 \frac{0.00030129 s^2 + 0.059398 s + 1}{s(0.074546 s + 1)} \quad (4.17)$$

$$G_{L\dot{\alpha}}(s) = 42212.79 \frac{0.00030129 s^2 + 0.059398 s + 1}{s(0.074546 s + 1)} \quad (4.18)$$

$$\begin{cases} \dot{x}_L = -13.42 x_L + 1 \cdot \dot{\alpha} \\ \Delta L = -10866.44 x_L + 170.61 \dot{\alpha} \end{cases} \quad (4.19)$$

b. 3-D pitching motion moment transfer function:

$$G_{C_M \dot{\alpha}}(s) = -0.05952 \frac{0.00071716 s^2 + 0.070537 s + 1}{s(0.078726 s + 1)} \quad (4.20)$$

$$G_{M \dot{\alpha}}(s) = -364921.09 \frac{0.00071716 s^2 + 0.070537 s + 1}{s(0.078726 s + 1)} \quad (4.21)$$

$$\begin{cases} \dot{x}_M = -12.70 x_M + 1 \cdot \dot{\alpha} \\ \Delta M = 80184.60 x_M - 3324.27 \dot{\alpha} \end{cases} \quad (4.22)$$

The combined unsteady aerodynamic model for the three-dimensional pitching motion with with amplitude $\alpha_0 = 1^\circ$ is written as:

$$\begin{cases} \dot{x}_L \\ \dot{x}_M \end{cases} = \begin{bmatrix} -13.42 & 0 \\ 0 & -12.70 \end{bmatrix} \begin{cases} x_L \\ x_M \end{cases} + \begin{bmatrix} 1 \\ 1 \end{bmatrix} \dot{\alpha} \quad (4.23)$$

$$\begin{cases} \Delta L \\ \Delta M \end{cases} = \begin{bmatrix} -10866.44 & 0 \\ 0 & 80184.60 \end{bmatrix} \begin{cases} x_L \\ x_M \end{cases} + \begin{bmatrix} 170.61 \\ -3324.27 \end{bmatrix} \dot{\alpha}$$

The Augmented 6x6 System Matrix

The 6x6 augmented system matrix for the plunging aerodynamic model is

$$\begin{bmatrix} -0.00658 & 17.83112 & 0.0 & -32.17 & 0.0 & 0.0 \\ -0.00012 & -0.85495 & 0.99725 & 0.0 & 0.00046 & 0.0 \\ 0.00001 & -3.43418 & -1.20526 & 0.0 & -0.00003 & 0.00581 \\ 0.0 & 0.0 & 1.0 & 0.0 & 0.0 & 0.0 \\ -0.08796-626.67835 & 730.98425 & 0.0 & 0.0 & -14.16921 & 0.0 \\ -0.08796-626.67835 & 730.98425 & 0.0 & 0.0 & 0.33718 & -13.30290 \end{bmatrix} \quad (4.24)$$

The 6x6 augmented system matrix for the pitching aerodynamic model is

$$\begin{bmatrix} -0.00658 & 17.83112 & 0.0 & -32.17 & 0.0 & 0.0 \\ -0.00012 & -0.85724 & 0.99985 & 0.0 & 0.00478 & 0.0 \\ 0.0 & -3.48332 & -1.14796 & 0.0 & -0.00001 & 0.06225 \\ 0.0 & 0.0 & 1.0 & 0.0 & 0.0 & 0.0 \\ -0.00012 & -0.85724 & 0.99985 & 0.0 & -13.40974 & 0.0 \\ -0.00012 & -0.85724 & 0.99985 & 0.0 & 0.00478 & -12.70232 \end{bmatrix} \quad (4.25)$$

The eigenanalysis of the above two system matrix are listed in Table 5 and 6.

The Difference Between the Rotary Oscillation and the Pure Pitching

In pure pitching motion of an airplane, the pitching angle θ varies while the angle of attack α stays constant. In pure plunging motion, the angle of attack changes but the pitching angle stays zero (Fig. 7) The term "rotary oscillation" that we use (as in ref. 12) means the sinusoidal pitching of the airfoil with respect to the wind, not to the horizontal line (Fig. 8). From the definition, it is clear that the plunging motion we considered is pure plunging motion, but the pitching we used both in the two-dimensional analysis and program H7WC is not pure pitching. That is, the oscillatory "rotation" of the airfoil is actually a combination of the pure pitching and a plunging motion. So some resolution will be needed if we want to consider the pure pitching motion.

rotary oscillation = pure pitching + pure plunging

ΔL due to pure pitching = ΔL due to rotary oscillation (present result) - ΔL due to the plunging motion part

ΔM due to pure pitching = ΔM due to rotary oscillation (present result) - ΔM due to the plunging motion part

From this idea, there is no problem to get the pure pitching motion frequency response as long as we have the corresponding rotary oscillation and plunging result. By doing so, it becomes complete in considering the three-dimensional longitudinal unsteady motion. Part of the result of pure pitching can be seen in Table 4.

CONCLUSIONS

In this thesis an approach of constructing the unsteady aerodynamic model from the frequency response calculation has been developed. This model has then been coupled to the aircraft longitudinal dynamic system to investigate the influence of the unsteady motion on the longitudinal modes. From the above analysis, it is obvious that the sinusoidal plunging and rotary oscillation both tend to destabilize the longitudinal modes of the aircraft. It has also verified the suspicion that the unsteady aerodynamics has more influence on the short period mode than on the phugoid mode. The unsteady motion decreases the damping of the aircraft but not the natural frequency. Unlike the easily controlled phugoid oscillation, the deterioration of damping in the short period mode can be of serious concern to the pilot. Because of the different natures of the short period and phugoid modes, the degrees of influence of the unsteady aerodynamic models on the two modes are also different. The unsteady plunging motion tends to affect the short period mode more than the rotary oscillation does (see Table 5). But, on the contrary, the rotary oscillation tends to have more influence on the phugoid mode than the plunging does.

Along with this analysis, we have a third mode (and a fourth mode in rotary oscillation) in the three-dimensional plunging case, which has a very high damping ($\zeta = 0.9998$) and a rather low frequency. We give it the name "aerodynamic mode" because it arises purely from the unsteady aerodynamics.

The numerical example given in this thesis are only for illustration. Because the incompleteness of the parameters and wing geometry, these ex-

amples can only serve as the indication of the influence of the unsteady aerodynamics on the aircraft longitudinal modes. If we have the complete parameters and wing geometry, whatever needed in the calculation, then we are able to calculate the influence of the unsteady aerodynamics more accurately. The system model of the whole aircraft longitudinal dynamics including the unsteady aerodynamics is shown in Figure 9. Here we have also shown only the pitch rate q enters the pure oscillatory pitching motion, while the total rate of angle of attack change excluding the contribution from pitch rate enters the pure plunging motion part.

In free flight condition, an unsteady motion usually consists of both pure pitching and plunging motion at the same time. For better illustrating the situation, we need to put in the unsteady aerodynamic model for both pitching and plunging. By doing so, we will have a higher order system than the present one. It will be a 7×7 matrix for the two-dimensional case and a 10×10 matrix for the three-dimensional case.

By noticing that the poles for the lift or moment transfer function in the three-dimensional plunging and rotary oscillation are almost the same, we can thus assume it to be so for convenience. That is, the lift transfer function has one same pole and moment transfer function has another same pole. Although this will slightly reduce the good matching between the data and the transfer function, but at the same time, we can get a lower order system which can reduce the complexity considerably. The simplified matrices will both be 6×6 in two-dimensional and three-dimensional cases. We will leave the reduction for the future.

REFERENCES

1. Bryan, G. H., "Stability in Aviation", Macmillan, London, 1911.
2. Wagner, H., "Über die Entstehung des dynamischen Auftriebes von Tragflügeln", Z. f. a. M. M., Bd. 5, Heft 1 Feb. 1925, S. 17-35.
3. Theodorsen, T., "General Theory of Aerodynamic Instability and the Mechanism of Flutter", T. R. 496, 1935, NACA.
4. Küssner, H. G., "Zusammenfassender Bericht über den instationären Auftrieb von Flügeln", Luftfahrtforschung, Bd. 13, Nr. 12, 20. Dec. 1936, S. 410-424.
5. Jones, R. T., "The Unsteady Lift of a Finite Wing", T. N. No. 682, 1939, NACA.
6. Jones, R. T., "Operational Treatment of the Non-Uniform Lift Theory in Airplane Dynamics", NACA TN 667, 1938.
7. Jones, R. T., "The Unsteady Lift of a Wing of Finite Aspect Ratio", NACA Rep. 681, 1940.
8. Etkin, B., "Dynamics of Flight", Wiley, New York, 1959.
9. Rodden, W. P. and Revell, J. D., "Status of Unsteady Aerodynamic Influence Coefficients", Paper FF-33, 1962, Institute of the Aeronautical Sciences; preprinted as Rept. TDR-930-(2230-09)TN-2, 1961, Aerospace Corp.
10. Ashley, H., Widnall, S. and Landahl, M. T., "New Directions in Lifting Surface Theory", AIAA Journal, Vol. 3, No. 1, Jan. 1965, pp. 3-16.
11. Landahl, M. T. and Stark, V. J. E., "Numerical Lifting-Surface Theory — Problems and Progress", AIAA Journal, Vol. 6, No. 11, Nov. 1968, pp. 2049-2060.
12. Tobak, M., "On the Use of the Indicial Function Concept in the Analysis of Unsteady Motions of Wings and Wing-tail Combinations", NACA Rep. 1188, 1954.
13. Durand, W. F., "Aerodynamic Theory", Vol. II, Division E, Durand Reprinting Committee, Pasadena, 1943.
14. Brogan, W. L., "Modern Control Theory", Quantum Publishing Inc., New York, 1974.
15. Etkin, B., "Dynamics of Atmospheric Flight", Wiley, New York, 1972.

16. Giesing, J. P., Kalman, T. P. and Rodden, W. P., "Subsonic Unsteady Aerodynamics for General Configurations , Part I, Vol. II _____ Computer Program H7WC", T. R. AFFDL-TR-71-5, Nov, 1971.
17. Stahl, B. et al., "Aerodynamic Influence Coefficients for Oscillating Planar Lifting Surfaces by the Doublet Lattice Method for Subsonic Flows Including Quasi-Steady Fuselage Interference", Rept. DAC-67201, Oct. 1968, McDonnell Douglas Corp.
18. Albano, E. and Rodden, W. P., "A Doublet-Lattice Method for Calculating Lift Distributions on Oscillating Surfaces in Subsonic Flows" , AIAA Journal, Vol. 7, No. 2, Feb. 1969, pp. 279-285; "errata", AIAA Journal, Vol. 7, NO. 11, Nov. 1969, p. 2192.

APPENDIX 1. A METHOD TO ACCURATELY LOCATE THE POLES AND ZEROS
OF THE TRANSFER FUNCTION FOR UNSTEADY AERODYNAMICS

1. If

$$G(s) = \frac{1}{s + \frac{1}{T}} \quad \text{then } \Delta\phi = -\tan^{-1} \omega T$$

2. If

$$G(s) = s + \frac{1}{T} \quad \text{then } \Delta\phi = \tan^{-1} \omega T$$

Before we use this method, we already have a transfer function with one pole and two zeros which can give the frequency response data shape. The disadvantage of the old transfer function is that it has a relatively higher error than expected. From inspecting the data, we know it is possible to have one pole at lower frequency and two zeros at higher frequencies. Let $\Delta\phi_p$, $\Delta\phi_{z_1}$, $\Delta\phi_{z_2}$ represent the phase angle changes due to the presence of pole p and zeros z_1 and z_2 , respectively.

$$\Delta\phi_p = -\tan^{-1} \frac{\omega}{p} = \tan^{-1} \left(-\frac{\omega}{p} \right)$$

$$\Delta\phi_{z_1} = \tan^{-1} \frac{\omega}{z_1}$$

$$\Delta\phi_{z_2} = \tan^{-1} \frac{\omega}{z_2}$$

Choose a frequency ω , and find the corresponding phase angle, then

$$\Delta\phi = \Delta\phi_p + \Delta\phi_{z_1} + \Delta\phi_{z_2}$$

and the problem becomes to solve the trigonometric equation:

$$\Delta\phi = \tan^{-1} \left(-\frac{\omega}{p} \right) + \tan^{-1} \left(\frac{\omega}{z_1} \right) + \tan^{-1} \left(\frac{\omega}{z_2} \right)$$

Since

$$\tan \Delta\phi_p = -\frac{\omega}{p} \quad (1)$$

$$\tan \Delta\phi_{z_i} = \frac{\omega}{z_i}$$

so

$$\begin{aligned} \tan \Delta\phi &= \tan(\Delta\phi_p + \Delta\phi_{z_1} + \Delta\phi_{z_2}) \\ &= \frac{\tan \Delta\phi_p + \tan(\Delta\phi_{z_1} + \Delta\phi_{z_2})}{1 - \tan \Delta\phi_p \tan(\Delta\phi_{z_1} + \Delta\phi_{z_2})} \end{aligned}$$

By using (1), and letting $\tan \Delta\phi = m$, we get

$$m \cdot (pz_1z_2) + \omega \cdot (z_1z_2 - pz_1 - pz_2) - m\omega^2 \cdot (p - z_1 - z_2) = \omega^3$$

or we can write

$$m \cdot \eta + \omega \cdot \chi - m\omega^2 \cdot \zeta = \omega^3$$

By picking three different ω 's and their corresponding $\Delta\phi$'s, we can solve η , χ , ζ . Now let $x_1 = p$, $x_2 = -z_1$, $x_3 = -z_2$, then

$$\eta = x_1x_2x_3$$

$$\chi = x_2x_3 + x_1x_2 + x_1x_3$$

$$\zeta = x_1 + x_2 + x_3$$

which will give the three coefficients of a cubic equation:

$$x^3 + a_1x^2 + a_2x + a_3 = 0 \quad (2)$$

where $a_1 = -\zeta$, $a_2 = \chi$, $a_3 = -\eta$. Solve for equation (2), we can get the pole and zeros easily.

Actually this method enables us to find any three pole-zero combinations without using other computer programs to calculate the cost function. This method can give a more accurate result than the least-squares method. By doing so, we are able to reduce the tedious work of matching polynomials to the data to a simple inverse-trigonometric analysis. One thing we have to be careful about is that the data points we choose for the calculation have some influence on the result. For the present case, we are only interested in the low frequency range ($\omega < 20$ rad/sec), so choosing all three data points in this range can assure a good approximation of the desired transfer function.

Another thing we should mention is that the whole idea of this method is trying to find the transfer function by a ratio of two polynomials. The polynomials are determined by finding their roots which correspond to the zeroes and poles of the frequency response plot. By inspection of the plot, the number of zeros and poles can be determined. From figure, it can be seen that there are two possible zeroes and one pole. Then, we employ the above method to accurately locate the positions of the pole and zeroes such that the ratio of these two polynomials give the same frequency response shape as the data.

¹ Here $s=i\omega$, $\Delta\phi$ is the phase shift and ω is the frequency of oscillation.

APPENDIX 2. GETTING THE TRANSFER FUNCTION FROM KNOWN
POLE AND ZEROS

Let

$$\begin{aligned} \frac{1}{T_p} &= p, & \frac{1}{T_{z_1}} &= z_1, & \frac{1}{T_{z_2}} &= z_2 \\ G_{C_L u}(s) &= K' \frac{(s + \frac{1}{T_{z_1}})(s + \frac{1}{T_{z_2}})}{s + \frac{1}{T_p}} \\ &= \frac{(K' \frac{z_1 z_2}{p}) [\frac{1}{z_1 z_2} s^2 + \frac{z_1 + z_2}{z_1 z_2} s + 1]}{\frac{1}{p} s + 1} \\ &= \frac{K(T_2 s^2 + T_3 s + 1)}{T_1 s + 1} \end{aligned}$$

where $T_1 = \frac{1}{p}, \quad T_2 = \frac{1}{z_1 z_2}, \quad T_3 = \frac{1}{z_1} + \frac{1}{z_2}$

and
$$G_{C_L u}(i\omega) = K \frac{1 + (T_1 T_3 - T_2)\omega^2}{1 + T_1^2 \omega^2} + i \frac{(T_3 - T_1)\omega + T_1 T_2 \omega^3}{1 + T_1^2 \omega^2}$$

The real part equals K when $\omega = 0$, and decreases when ω increases. The imaginary part starts from zero, first decreases then increases when ω increases. By suitable choice of K (using least-squares method), we can get a very good approximation of the transfer function representing unsteady aerodynamics. In the frequency range we are most interested in, the error between the transfer and the data can be less than 0.1%.

APPENDIX 3. AN EXAMPLE CASE TO FIND THE POLE AND ZEROS
OF AN TRANSFER FUNCTION

In this appendix, we follow the method depicted in Appendix 2 and 3. The transfer function used is the one that represents the three-dimensional pitching lift. The three frequencies we choose are

$$\omega_i = 1, 10, 30$$

and the corresponding phase shifts are

$$\phi_i = -0.863^\circ, -5.219^\circ, 1.846^\circ$$

Let $m_i = \tan \phi_i$, we get

$$m_1 = \tan \phi_1 = -0.015064$$

$$m_2 = \tan \phi_2 = -0.091336$$

$$m_3 = \tan \phi_3 = 0.032236$$

Let

$$pz_1z_2 = \eta$$

$$z_1z_2 - pz_1 - pz_2 = \chi$$

$$p - z_1 - z_2 = \zeta$$

then the three equations are:

$$\left\{ \begin{array}{l} -0.015064 \quad \eta + 1 \quad \chi + 0.015064 \quad \zeta = 1 \\ -0.091336 \quad \eta + 10 \quad \chi + 9.1336 \quad \zeta = 1000 \\ 0.032236 \quad \eta + 30 \quad \chi - 29.0124 \quad \zeta = 27000 \end{array} \right.$$

Solving three equations, we get

$$\eta = 44523.93$$

$$\chi = 674.48$$

$$\zeta = -183.73$$

then

$$a_1 = -\zeta = 183.73$$

$$a_2 = \chi = 674.48$$

$$a_3 = -\eta = -44523.93$$

and give the cubic equation:

$$x^3 + 183.73 x^2 + 674.48 x - 44523.93 = 0$$

Use Newton-Raphson method to get the roots:

$$x_1 = 13.41452$$

$$x_2 = -18.58839$$

$$x_3 = -178.55687$$

which give the one pole and two zeros as expected:

$$p = 13.41452$$

$$z_1 = -18.58839$$

$$z_2 = -178.55687$$

APPENDIX 4. THE DERIVATION OF THE NEW AUGMENTED SYSTEM EQUATIONS

1. The \dot{V} equation is unchanged.

2. The $\dot{\alpha}$ equation:

From Etkin's (5.10,10(b)) and 5.10,18-(b) and (d):

$$mV_e \dot{\gamma} = \Delta T \sin \alpha_T + \Delta \alpha T_e \cos \alpha_T + \Delta L + m g \sin \gamma_e \Delta \gamma$$

where $\Delta L = L_V \Delta V + L_\alpha \Delta \alpha + L_q q + \Delta L_C + \text{unsteady lift part}$

$$\Delta T = T_V \Delta V + \Delta T_C$$

$$\Delta \gamma = \Delta \theta - \Delta \alpha$$

we get

$$mV_e (\dot{\theta} - \dot{\alpha}) = (T_V \Delta V + \Delta T_C) \sin \alpha_T + \Delta \alpha T_e \cos \alpha_T + m g \sin \gamma_e (\Delta \theta - \Delta \alpha) \\ + L_V \Delta V + L_\alpha \Delta \alpha + L_q q + \text{unsteady lift part} + \Delta L_C$$

$$(-mV_e) \dot{\alpha} = (L_V + T_V \sin \alpha_T) \Delta V \\ + (T_e \cos \alpha_T - m g \sin \gamma_e + L_\alpha) \Delta \alpha \\ + (-mV_e + L_q) q \\ + (m g \sin \gamma_e) \Delta \theta \\ + \text{unsteady lift part} \\ + (\Delta L_C + \Delta T_C \sin \alpha_T)$$

$$-mV_e \dot{\alpha} = (L_V + T_V \sin \alpha_T) \Delta V \\ + (T_e \cos \alpha_T - m g \sin \gamma_e + L_\alpha) \Delta \alpha \\ + (-mV_e + L_q) q \\ + (m g \sin \gamma_e) \Delta \theta \\ + c_1' x + d_1' \dot{\alpha}$$

$$+ (\Delta L_C + \Delta T_C \sin \alpha_T)$$

Rearrange, we get

$$\begin{aligned} \dot{\alpha} = & \left(- \frac{L_V + T_V \sin \alpha_T}{mV_e + d_1'} \right) & \Delta V \\ & + \left(- \frac{T_e \cos \alpha_T - mgsin \gamma_e + L_\alpha}{mV_e + d_1'} \right) & \Delta \alpha \\ & + \left(\frac{mV_e - L_q}{mV_e + d_1'} \right) & q \\ & + \left(- \frac{mgsin \gamma_e}{mV_e + d_1'} \right) & \Delta \theta \\ & + \left(- \frac{c_1'}{mV_e + d_1'} \right) & x_a \\ & + \left(- \frac{\Delta L_C + \Delta T_C \sin \alpha_T}{mV_e + d_1'} \right) \end{aligned}$$

3. The \dot{q} equation:

From 5.10,10(c), 5.10,18(c),

$$I_y \dot{q} = M_V \Delta V + M_\alpha \Delta \alpha + M_q q + \Delta M_C + \text{unsteady moment part}$$

$$I_y \dot{q} = M_V \Delta V + M_\alpha \Delta \alpha + M_q q + \Delta M_C + c_2' x_a + d_2' \cdot \dot{\alpha}$$

Rearrange, we get

$$\begin{aligned} \dot{q} = & \frac{1}{I_y} \left[M_V - \frac{d_2' (L_V + T_V \sin \alpha_T)}{mV_e + d_1'} \right] & \Delta V \\ & + \frac{1}{I_y} \left[M_\alpha - \frac{d_2' (L_\alpha + T_e \cos \alpha_T - mgsin \gamma_e)}{mV_e + d_1'} \right] & \Delta \alpha \\ & + \frac{1}{I_y} \left[M_q + \frac{d_2' (mV_e - L_q)}{mV_e + d_1'} \right] & q \\ & + \frac{1}{I_y} \left[- \frac{d_2' (mgsin \gamma_e)}{mV_e + d_1'} \right] & \Delta \theta \end{aligned}$$

$$\begin{aligned}
 & + \frac{1}{I_y} \left[c_2' - \frac{d_2' \cdot c_1'}{mV_e + d_1'} \right] \\
 & + \frac{1}{I_y} \left[\Delta M_C - \frac{d_2' \cdot \Delta L_C}{mV_e + d_1'} \right]
 \end{aligned}
 \quad x_a$$

4. The new \dot{x}_a equation:

$$\begin{aligned}
 \dot{x}_a &= a' x_a + V_e \cdot \dot{\alpha} \\
 &= V_e A_{21}' \quad \Delta V \\
 &+ V_e A_{22}' \quad \Delta \alpha \\
 &+ V_e A_{23}' \quad q \\
 &+ V_e A_{24}' \quad \Delta \theta \\
 &+ (a' + V_e A_{25}') x_a
 \end{aligned}$$

APPENDIX 5. SOME DATA USED IN THE NUMERICAL EXAMPLE

$$\begin{array}{ll}
 W = 100,000 \text{ lbs} & \bar{S} = 1667 \text{ ft}^2 \\
 \bar{c} = 15.4 \text{ ft} & W/\bar{S} = 60 \text{ psf} \\
 AR = 7 & \rho_e \text{ at } 30,000 \text{ ft} = 0.000889 \text{ slug/ft}^3 \\
 V_e = 500 \text{ mph} = 733 \text{ fps} & \mu = 272 \\
 \hat{I}_y = 7 & I_y = 1288180 \text{ slug-ft}^2 \\
 C_{L_e} = C_{W_e} = 0.25 & C_{D_e} = 0.0188 \\
 C_D = 0.016 + \frac{C_{L_e}^2}{7} & C_{L_\alpha} = 4.88 \\
 C_{m_\alpha} = 4.88 (h_n - h') & h_n - h' = 0.15 \\
 C_{D_\alpha} = \frac{2C_{L_e}}{7} C_L = 0.111 & C_{L_{\dot{q}}} = 0 \\
 C_{m_{\dot{q}}} = -22.9 & C_{T_V} = -2C_{T_e} = -2C_{D_e} \\
 C_{L_V} = C_{D_V} = C_{M_V} = 0 & L_\alpha = \rho \bar{c} \bar{V}^2 b = 2501470 \text{ lbs/rad.} \\
 M_\alpha = -4487940 (\text{from } C_{m_\alpha}) \text{ lb-ft/rad.} & m = 3103.82 \text{ slug} \\
 L_V = \rho \bar{V} \bar{S} C_{L_e} = 271.57 \text{ lb-sec/ft} & h' = 0.1335
 \end{array}$$

APPENDIX 6. LINEAR TRANSFORMATION OF THE SYSTEM MATRICES

Let \hat{x} represent the non-dimensional state variable $[\Delta\hat{V}, \Delta\alpha, \hat{q}, \Delta\theta]^T$, x represent the dimensional state variable $[\Delta V, \Delta\alpha, q, \Delta\theta]^T$, and

$$\dot{\hat{x}} = \hat{A} \hat{x} + \hat{B} \Delta\delta_e$$

$$\dot{x} = A x + B \Delta\delta_e$$

where

$$\hat{x} = \begin{pmatrix} \Delta\hat{V} \\ \Delta\alpha \\ \hat{q} \\ \Delta\theta \end{pmatrix} = \begin{pmatrix} \frac{1}{V_e} & 0 & 0 & 0 \\ 0 & 1 & 0 & 0 \\ 0 & 0 & \frac{\bar{c}}{2V_e} & 0 \\ 0 & 0 & 0 & 1 \end{pmatrix} \begin{pmatrix} \Delta V \\ \Delta\alpha \\ q \\ \Delta\theta \end{pmatrix} = T' x$$

$$\dot{\hat{x}} = \begin{pmatrix} D\hat{V} \\ D\alpha \\ D\hat{q} \\ D\theta \end{pmatrix} = \begin{pmatrix} \frac{\bar{c}}{2V_e} & 0 & 0 & 0 \\ 0 & \frac{\bar{c}}{2V_e} & 0 & 0 \\ 0 & 0 & (\frac{\bar{c}}{2V_e})^2 & 0 \\ 0 & 0 & 0 & \frac{\bar{c}}{2V_e} \end{pmatrix} \begin{pmatrix} \dot{\hat{V}} \\ \dot{\alpha} \\ \dot{\hat{q}} \\ \dot{\theta} \end{pmatrix} = T \dot{x}$$

Combine all these equations together, we have the following relation:

$$\begin{aligned} \dot{x} &= T^{-1} \dot{\hat{x}} \\ &= T^{-1} (\hat{A} \hat{x} + \hat{B} \Delta\delta_e) \\ &= (T^{-1} \hat{A} T') x + (T^{-1} \hat{B}) \Delta\delta_e \\ &= A x + B \Delta\delta_e \end{aligned}$$

So we have

$$A = T^{-1} \hat{A} T' \quad \text{and} \quad B = T^{-1} \hat{B}$$

In our example,

$$T = \begin{pmatrix} 0.00001433 & 0.0 & 0.0 & 0.0 \\ 0.0 & 0.010504 & 0.0 & 0.0 \\ 0.0 & 0.0 & 0.000113 & 0.0 \\ 0.0 & 0.0 & 0.0 & 0.010504 \end{pmatrix}$$

$$T' = \begin{pmatrix} 0.001364 & 0.0 & 0.0 & 0.0 \\ 0.0 & 1.0 & 0.0 & 0.0 \\ 0.0 & 0.0 & 0.010504 & 0.0 \\ 0.0 & 0.0 & 0.0 & 1.0 \end{pmatrix}$$

$$T^{-1} = \begin{pmatrix} 69783.67 & 0.0 & 0.0 & 0.0 \\ 0.0 & 95.2018 & 0.0 & 0.0 \\ 0.0 & 0.0 & 9066.1831 & 0.0 \\ 0.0 & 0.0 & 0.0 & 95.2018 \end{pmatrix}$$

Table 1. The Comparison Between the Approximated Transfer Function
for the Three-Dimensional Plunging Lift and the Data from H7WC.

ω	k	$ C_L $ from transfer function	$ C_L $ from program H7WC	error
1	0.0105	0.008274	0.008274	0.00%
3	0.0315	0.0081847	0.0081812	0.04%
5	0.0525	0.0080239	0.0080311	-0.09%
10	0.1050	0.0074742	0.0075378	-0.8 %
15	0.1575	0.0069549	0.0070281	-1.04%

Table 2. The Lift and Moment Coefficients in the Three-Dimensional Unsteady Motions.

ω	k	pitching		plunging	
		C_L/α_0	C_M/α_0	C_L/u_0	C_M/u_0
1	0.0105	-0.105883+10.001595	0.059437-10.000481	-0.008272+10.000165	0.004644-10.000074
3	0.0315	-0.104690+10.004434	0.058798-10.001247	-0.008168+10.000465	0.004588-10.000206
5	0.0525	-0.102747+10.006569	0.057769-10.001630	-0.008000+10.000706	0.004499-10.000306
10	0.1050	-0.096687+10.008831	0.054612-10.000936	-0.007465+10.001045	0.004220-10.000415
15	0.1575	-0.090923+10.007823	0.051693+10.001491	-0.006942+10.001097	0.003953-10.000373
20	0.2100	-0.086339+10.005004	0.049474+10.004854	-0.006511+10.000985	0.003740-10.000245

Table 3. The Poles and Zeroes of the Transfer Function in 2-D and 3-D Cases.

	case	pole	1st zero	2nd zero
1	2-D plunging motion lift part	5.90	9.01	182.24
2	2-D pitching motion lift part	6.34	8.89	147.19
3	3-D plunging motion lift part	14.17	21.45	254.90
4	3-D plunging motion moment part	13.54	19.30	166.64
5	3-D pitching motion lift part	13.42	18.59	178.56
6	3-D pitching motion moment part	12.70	17.18	81.18

Table 4. The Lift and Moment Coefficients in the Three-Dimensional Sinusoidal Pure Pitching Motion.

$$(\theta = \theta_0 \cos \omega t)$$

ω	k	C_L/θ_0	C_M/θ_0
1	0.0105	-0.000062-i0.000511	0.000035+i0.000468
3	0.0315	-0.000179-i0.001510	0.000096+i0.001392
5	0.0525	-0.000391-i0.002458	0.000208+i0.002288

Table 5. The Eigenanalysis of Quasi-Steady System Matrix and Augmented System Matrices When Including Different Unsteady Aerodynamic Effects.

case mode		quasi-steady case	2-D plunging motion only	2-D pitching motion only	3-D pitching motion only	3-D plunging motion only
short period	λ'	-1.107±i1.801	-0.884±i1.958	-1.000±i1.858	-1.000±i1.862	-0.856±i1.926
	ζ'	0.5236	0.4113	0.4740	0.4733	0.4061
	ω_n	2.114	2.148	2.110	2.114	2.108
phugoid	λ'	-0.002909 ±i0.05507	-0.002877 ±i0.05481	-0.002890 ±i0.05475	-0.002806 ±i0.05673	-0.002873 ±i0.05500
	ζ'	0.05275	0.05242	0.05270	0.04940	0.05216
	ω_n	0.05514	0.05489	0.05483	0.05680	0.05508
aerodynamic mode 1		—	-5.788	-6.338	-13.41	λ' -13.91±i0.2431
						ζ' 0.9998
						ω_n 13.91
aerodynamic mode 2		—	—	—	-12.71	—

Table 6. Comparison of Some Useful Measures of the Rate of Growth or Decay of the Oscillation.

mode	measures		period (sec)	$t_{1/2}$ (sec)	$N_{1/2}$ (cycles)
	case				
short period	1.	quasi-steady case	3.49	0.626	0.18
	2.	2-D case when including plunging motion only	3.21	0.784	0.24
	3.	2-D case when including pitching motion only	3.38	0.693	0.20
	4.	3-D case when including plunging motion only	3.26	0.810	0.25
	5.	3-D case when including pitching motion only	3.37	0.693	0.21
phugoid	1.	quasi-steady case	114.1	238.2	2.08
	2.	2-D case when including plunging motion only	114.6	240.88	2.10
	3.	2-D case when including pitching motion only	114.8	239.79	2.08
	4.	3-D case when including plunging motion only	114.2	241.21	2.11
	5.	3-D case when including pitching motion only	110.8	246.97	2.22

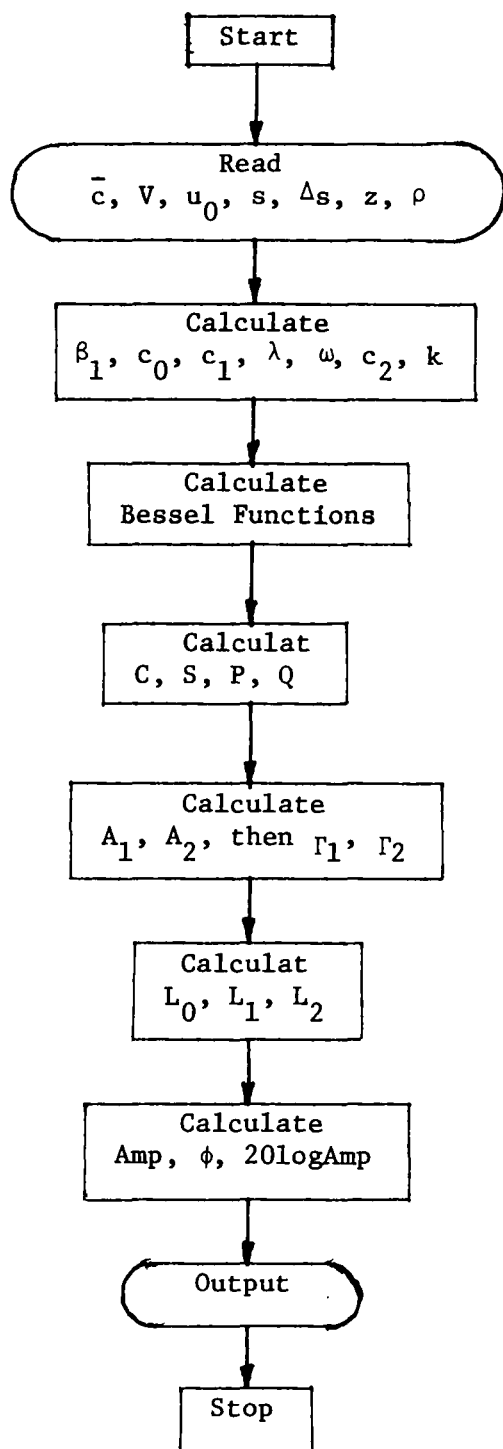


Figure 1. The Flow Chart for the Two-Dimensional Lift Calculation.

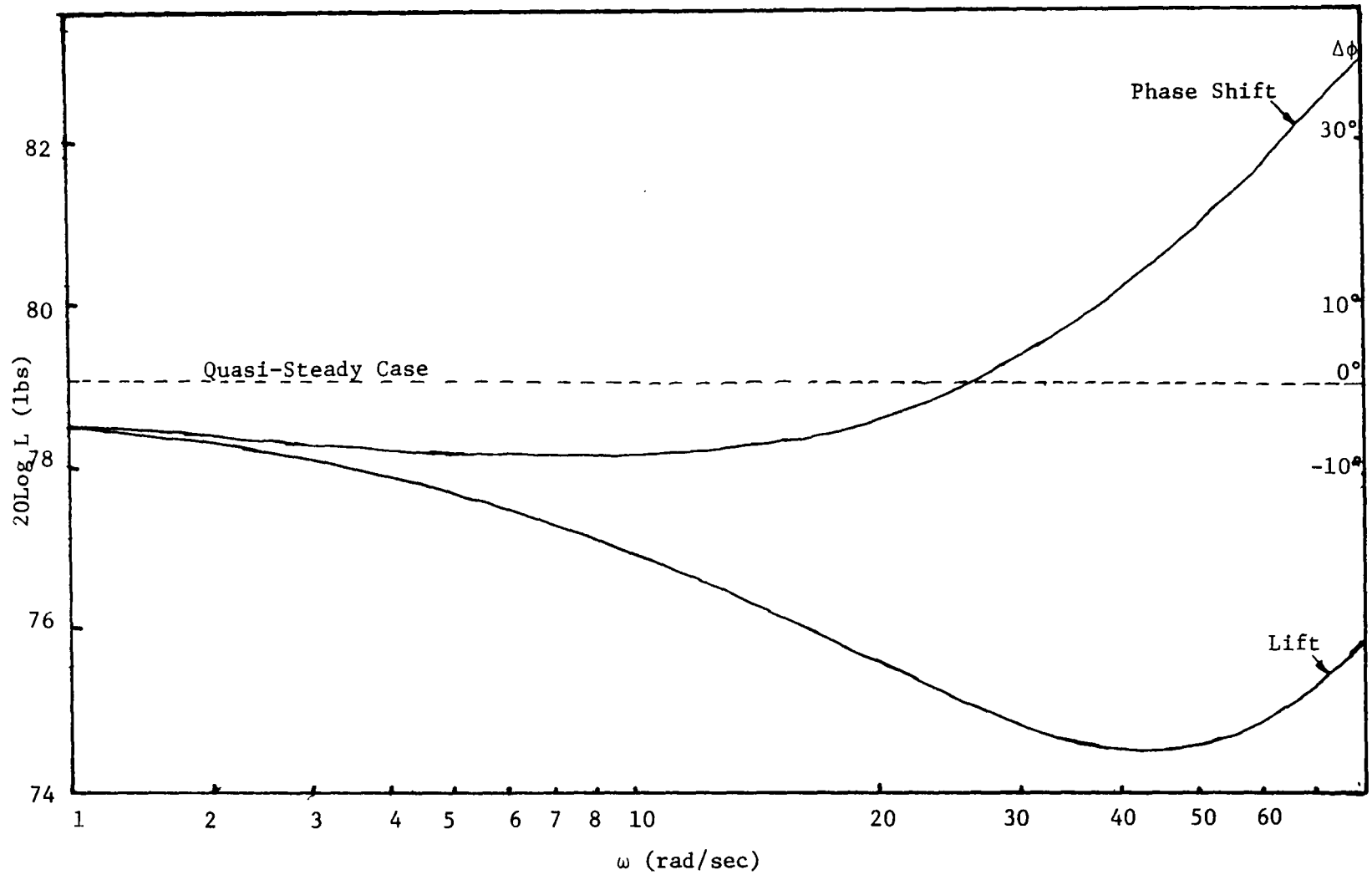
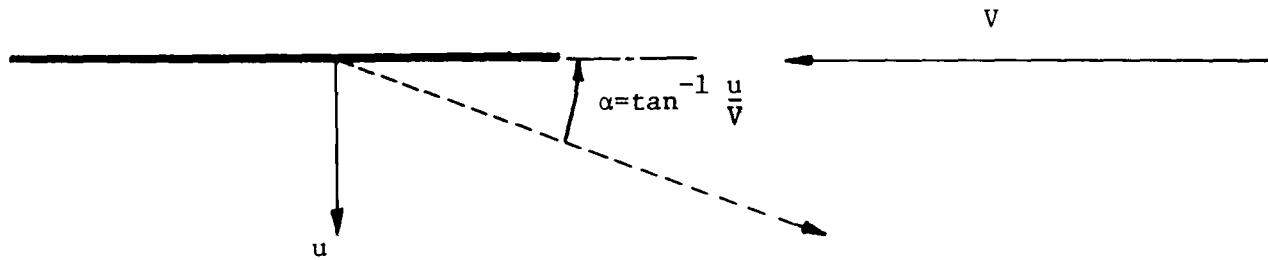


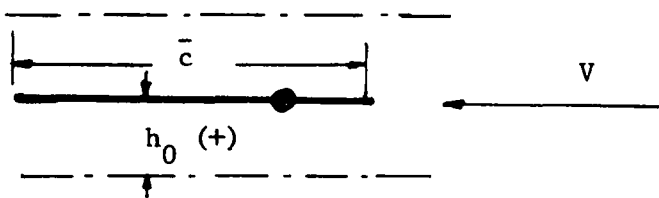
Figure 2. The Bode Plot of the Lift Frequency Response in Two-Dimensional Plunging Motion Case.



$$h = h_0 \cos \omega t$$

$$u = u_0 \sin \omega t$$

Figure 3. Sinusoidal Plunging Motion of the Airfoil in the Two-Dimensional Case.

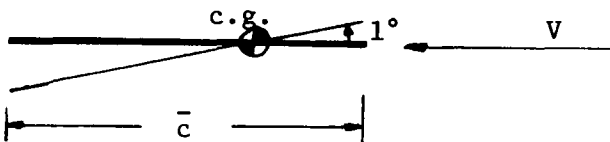


$$h = \text{Re}(h_0 e^{i\omega t})$$

$$u = \text{Re}(i\omega h_0 e^{i\omega t})$$

$$h_0 = \frac{u_0}{\omega} = \frac{12}{\omega}$$

Figure 4(a). The Sinusoidal Plunging Motion and Its Representation Used in the Program H7WC.



$$\frac{h}{s} = -0.0043035 + 0.01745 \frac{x}{s}$$

s = semispan (in inch)

h = vertical displacement from the x-y plane of wind axes (in inch)

Figure 4(b). The Sinusoidal Pitching Motion and Its Representation Used in the Program H7WC.

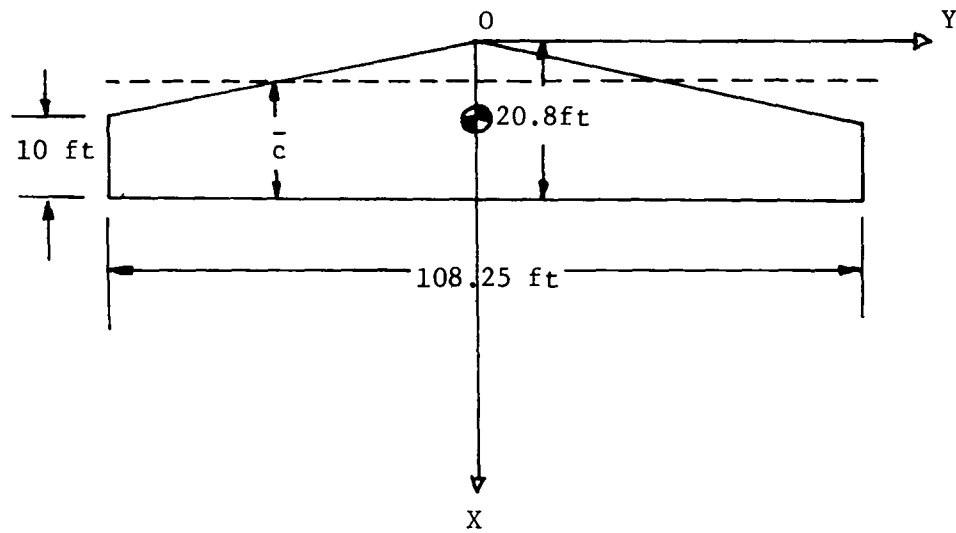


Figure 5. The Wing Geometry Used in the Program H7WC.

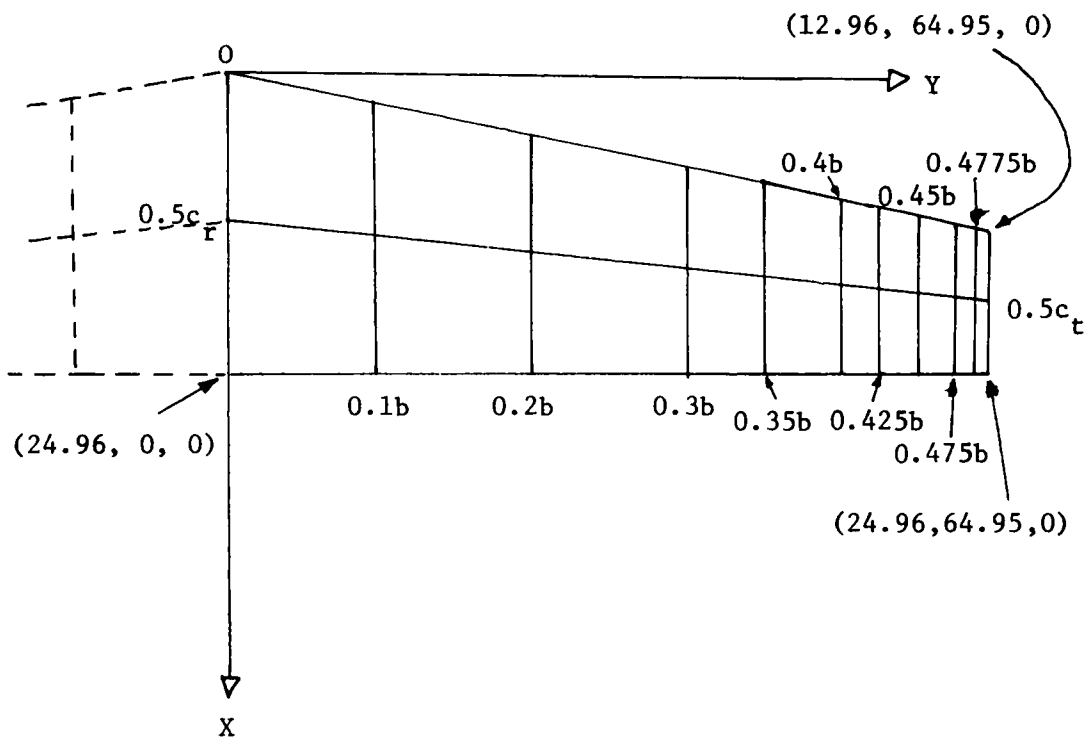
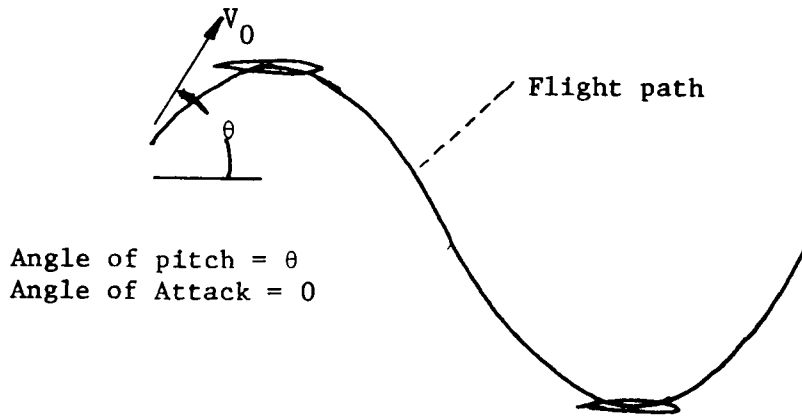
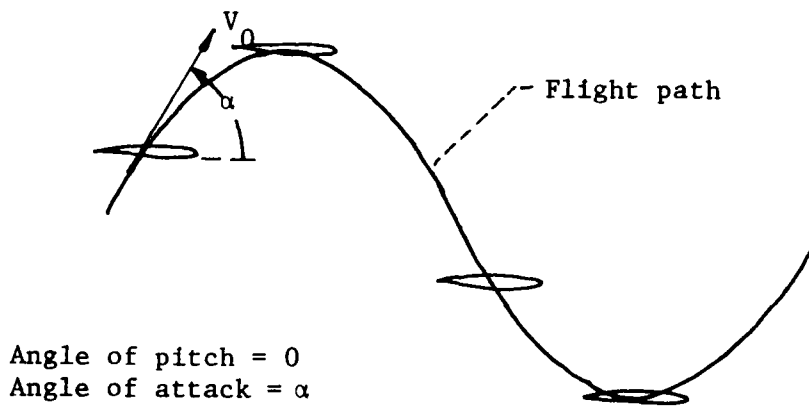


Figure 6. The Division of Strips and Boxes and Their Coordinates Used in the Program H7WC.



(a)



(b)

Figure 7. The Motion due to (a) Pitching Angle Change, and (b) Angle of Attack Change.

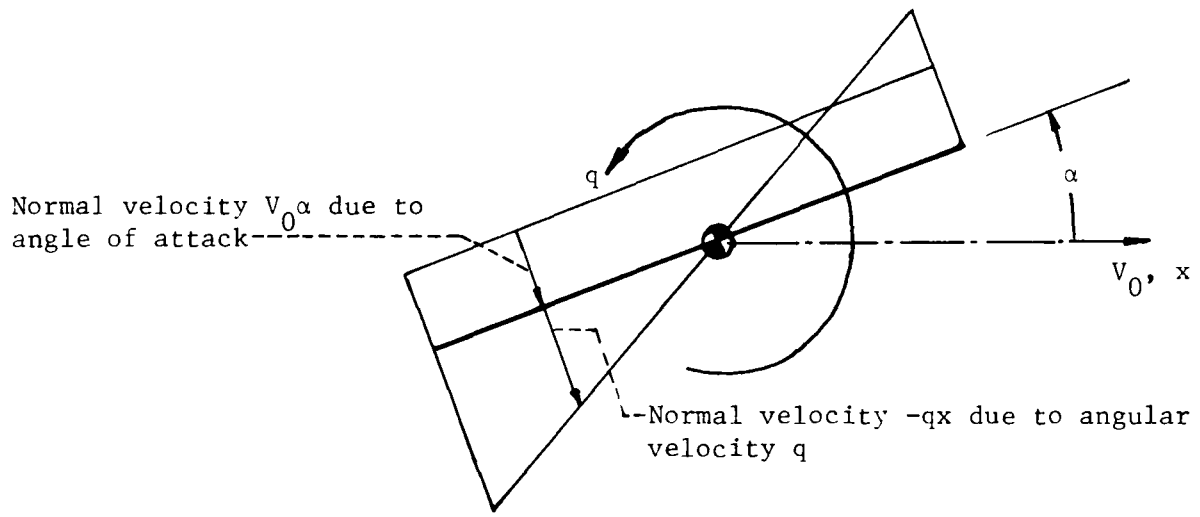


Figure 8. The Rotary Oscillation in Free Flight Condition.

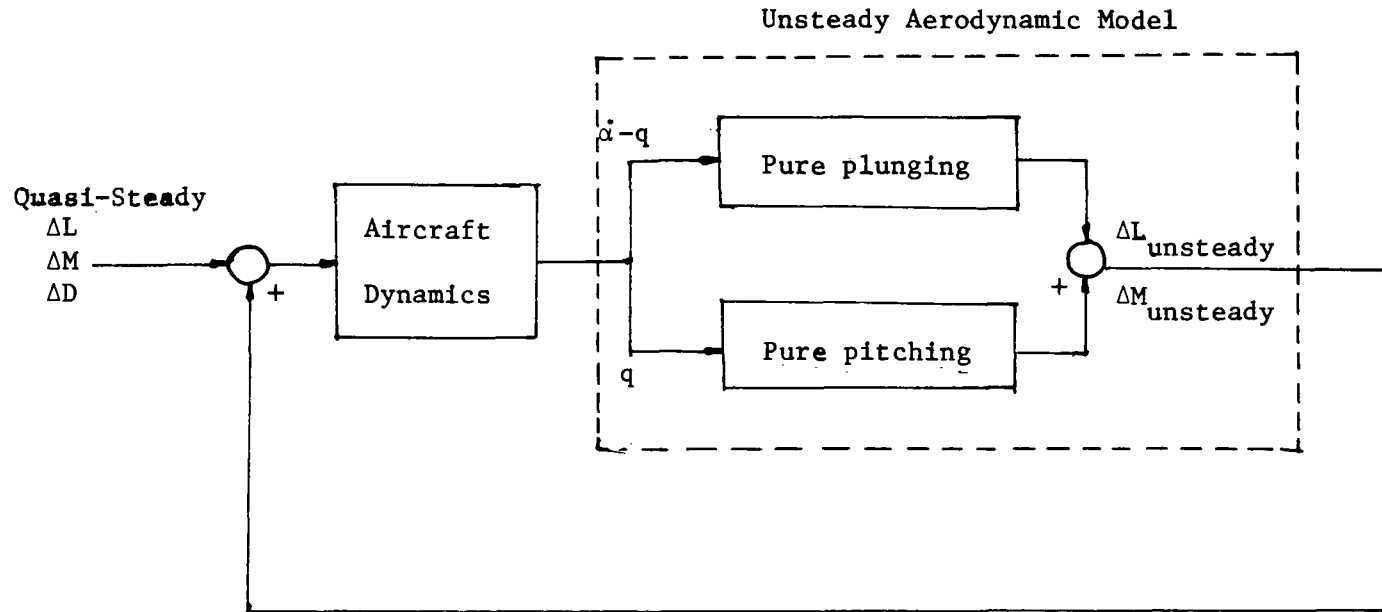


Figure 9. The Block Diagram of Coupling the Unsteady Aerodynamic Model to the Quasi-steady Aircraft System.

**The vita has been removed from
the scanned document**

THE LONGITUDINAL DYNAMICS OF A RIGID AIRCRAFT
INCLUDING UNSTEADY AERODYNAMIC EFFECTS

by

Ta Kang Chen

(ABSTRACT)

The main object of this thesis is to give an introductory study of the longitudinal motion of an aircraft, including some effects of non-uniform motion. Because this subject is connected with practical problems of importance in the domain of applied aerodynamics and control, a great effort has been given to setting up the physics of unsteady aerodynamics and its effects on the aircraft longitudinal modes. Numerical examples are given for both the two-dimensional and three-dimensional rigid wing, subsonic case. In this research, from the unsteady aerodynamic theory, through the frequency response calculation, system identification and the augmentation of the aircraft dynamic system, a carefully derived theory and a computer algorithm have been presented and used.

It is our main purpose that a suitable unsteady aerodynamic transfer function be obtained and be coupled to the aircraft quasi-steady dynamic system. A new modified model which includes the unsteady aerodynamic effects has been constructed and been compared with the conventional model and the differences between them have been discussed.